Rhythmic Perception:
New evidence for rhythmicity of behavioural and neuronal signatures

Inaugural-Dissertation

zur Erlangung des Doktorgrades
der Mathematisch-Naturwissenschaftlichen Fakultät
der Heinrich-Heine-Universität Düsseldorf

vorgelegt von

Michelle Johannknecht
aus Lippstadt

Düsseldorf, Juni 2024

aus dem Institut für Klinische Neurowissenschaften und medizinische Psychologie
der Heinrich-Heine-Universität Düsseldorf

Gedruckt mit der Genehmigung der
Mathematisch-Naturwissenschaftlichen Fakultät der
Heinrich-Heine-Universität Düsseldorf

Berichterstatter:

1. PD Dr. Joachim Lange

2. Prof. Dr. Christan Bellebaum

Tag der mündlichen Prüfung: 02.07.2025
(bitte bei der Abgabe Ihrer Dissertation noch offenlassen)

Table of contents

Zusammenfassung

Unsere visuelle Wahrnehmung scheint ein kontinuierlicher Zustrom von Informationen zu sein. Jedoch sehen wir auch einen kontinuierlichen Strom an Informationen, wenn das Gesehene eine schnelle Abfolge diskreter Bilder ist. Es wird angenommen, dass neuronale Oszillationen der zugrundeliegende Mechanismus ist, der unsere visuelle Wahrnehmung prägt. Die Idee ist, dass das menschliche visuelle System nicht kontinuierlich arbeitet. Bei der rhythmischen Wahrnehmung wird davon ausgegangen, dass die Phase der Oszillation die Wahrscheinlichkeit bestimmt, schwache Reize wahrzunehmen. Bei der diskreten Wahrnehmung wird davon ausgegangen, dass die Frequenz der Oszillation ein verbindliches Fenster schafft, in dem visuelle Ereignisse zeitlich integriert werden. In einer visuellen Integrationsaufgabe untersuchte ich, wie die neuronale Oszillation die visuelle Wahrnehmung bei jungen gesunden Probanden beeinflusst.

In der ersten Studie führte ich eine Magnetoenzephalographie-Studie durch, bei der ich die neuronale Oszillation aufzeichnete, während ich den Teilnehmern gleichzeitig eine Verhaltensaufgabe stellte bei der zwei Bilder zeitlich integriert werden müssen. Bei der Analyse der neuronalen Oszillation vor der Aufgabe stellte ich fest, dass sich die Phase der neuronalen Oszillation zwischen richtigen und falschen Antworten unterscheidet. Diese Phaseneffekte traten mehrere hundert Millisekunden vor der Verhaltensaufgabe auf (500 ms vor bis zu 800 ms). Die Frequenz dieser Phaseneffekte war zwischen 6 und 20 Hz. Darüber hinaus stand das Verhalten in direktem Zusammenhang mit dem momentanen Phasenwinkel der neuronalen Oszillation vor der Aufgabe. Diese Studie untersuchte in erster Linie den Einfluss der neuronalen Oszillation auf die Fähigkeit, zwei Bilder zu integrieren. Diese Studie legte den Grundstein für meine zweite Studie.

In Studie zwei habe ich versucht, die zugrundeliegende Oszillation zu modulieren, indem ich vor der eigentlichen Integrationsaufgabe einen unterschwelligen Stimulus präsentierte. Ein unterschwelliger Stimulus ist ein Stimulus, der vom Teilnehmer nicht bewusst wahrgenommen wird, aber physisch vorhanden ist. Ich verwendete die gleiche visuelle Integrationsaufgabe wie in Studie eins. Während dieses Experiments modulierte ich die Zeit zwischen dem unterschwelligen Stimulus und der Verhaltensaufgabe, um die zugrunde liegende neuronale Oszillation systematisch zu verändern. Ich analysierte die Verhaltensdaten in Abhängigkeit von der Zeitverzögerung zwischen dem unterschwelligen Reiz und der Verhaltensaufgabe. Als

Ergebnis beobachtete ich rhythmische Fluktuationen der Verhaltensdaten in einem unteren Frequenzbereich (unter 5 Hz), zwischen 10 und 13 Hz und zwischen 17 und 24 Hz.
Die Ergebnisse beider Studien deuten darauf hin, dass die neuronalen Oszillationen unsere visuelle Wahrnehmung prägen. Ich fand Hinweise dafür, dass unsere visuelle Integrationsfähigkeit ein rhythmischer Prozess ist, der durch die momentane Phase der Oszillation moduliert wird. In Studie zwei war ich in der Lage, die zugrundeliegende Oszillation zu modulieren und so weitere kausale Beweise für die wichtige Rolle der Phase der neuronalen Oszillation in unserer visuellen Wahrnehmung zu sammeln.

Abstract

Our visual perception seems to be a continuous influx of information. However, we see a continuous stream of information when we observe discrete images one after the other in fast succession. Neuronal oscillations are believed to be the underlying mechanism shaping our visual perception. The idea is that the human visual system operates in a non-continuous manner. Rhythmic perception assumes that the phase of the ongoing oscillation defines the likelihood of perceiving weak stimuli. Discrete perception assumes that the frequency of the oscillation creates a binding window, where visual events are integrated over time. In a visual integration task, I investigated how neuronal oscillation shapes visual perception in young healthy participants.

In the first study, I conducted a magnetoencephalography study, recording the neuronal oscillation while simultaneously presenting a behavioural integration task to the participants. Analysing the neuronal oscillation prior to the task, I found that the phase of the neuronal oscillation differs between correct and incorrect trials. These phase effects were several hundred milliseconds prior to the behavioural task (500 ms before up to 800 ms). The frequency of these phase effects ranged between 6 and 20 Hz. In addition, the behaviour was directly related to the momentary phase angle of the neuronal oscillation prior to the observed task. This study primarily analysed the influence of neuronal oscillation on the ability to integrate two images into one percept. This study laid the groundwork for my second study.

In study two, I tried to modulate the underlying oscillation by presenting a subliminal stimulus prior to the actual integration task. A subliminal stimulus is a stimulus that is not consciously perceived by the participant but is physically present. I used the same visual integration task as in study one. During this experiment, I modulated the time between the subliminal stimulus and the test stimulus to systematically change the underlying neuronal oscillation. I analysed the behavioural data as a function of the time delay between the subliminal stimulus and the test stimulus. As a result, I observed rhythmic fluctuation of the behavioural response in a lower frequency range (below 5 Hz), between 10 and 13 Hz, and between 17 and 24 Hz.

The results of both studies indicate that underlying neuronal oscillation shapes our visual perception. I found evidence that our visual integration ability is a rhythmic process modulated by the momentary phase of the oscillation. In study two specifically, I was able to modulate the underlying oscillation, collecting more causal evidence for the important role of the phase of neuronal oscillation in our visual perception.

Introduction

Our visual system provides us with a seemingly continuous stream of information. Therefore, our perception of the surroundings seems uninterrupted. However, visual illusions challenge this view. Our perception changes while the physical input is constant. This indicates that there could be an underlying process influencing our perception. How does this process influence our perception? Moreover, what is the underlying mechanism of this process? In this thesis, I investigated the driving force of our perception in an experimental setting where participants had to integrate two complementary visual stimuli over time. I assume the underlying force is oscillations generated by neurons in different brain areas. In the introduction of this thesis, I will explain the theoretical groundwork needed to understand the following studies. In Chapter 1, I introduce the neuron and its functionalities and explain how neurons transmit information in the brain. In Chapter 2, I explain how neurons produce oscillations. Chapter 3 briefly introduces the visual system and how it processes visual information. Afterwards, in chapter 4, there is an introduction to the theoretical framework of periodic perception. Finally, Chapter 5 will introduce the measurement method magnetoencephalography (MEG), which I used in this thesis to measure neuronal signals.

Neurons

A neuron is a negatively charged cell with a semipermeable membrane that can receive and pass on electrical signals (Pinel et al., 2017; Sadava et al., 2011). Its main functions are to receive input, integrate it over time and space, transfer it over a physical distance, and generate an output to other connected cells (Buzsáki, 2006; Sadava et al., 2011).

The functional units of a neuron are the dendrites, the soma, the axon and the axon terminal. The dendrites receive information and are connected to other neurons (Sadava et al., 2011). The soma contains the cell nucleus and other cellular organelles (Sadava et al., 2011). The axon transfers the signal and functions as an insulated cable with gaps in between. The insulation comes from myelin, a biomembrane that inhibits electric flow. The gaps in between are called nodes of Ranvier; here, electrical flow across the membrane is possible. This insulation facilitates signal transfer (Sadava et al., 2011).

The axon terminal transfers the electrical signal to the following cells (Sadava et al., 2011) (see Figure 1). Researchers categorise cortical neurons into pyramid cells and stellate cells. Pyramid cells are multipolar (multiple dendrites) with pyramid-shaped cell bodies and long dendrites running parallel through the cortex (Pinel et al., 2017). Stellate cells are star-shaped neurons that work mainly as interneurons. They connect multiple neurons and have short but many dendrites (Pinel et al., 2017).

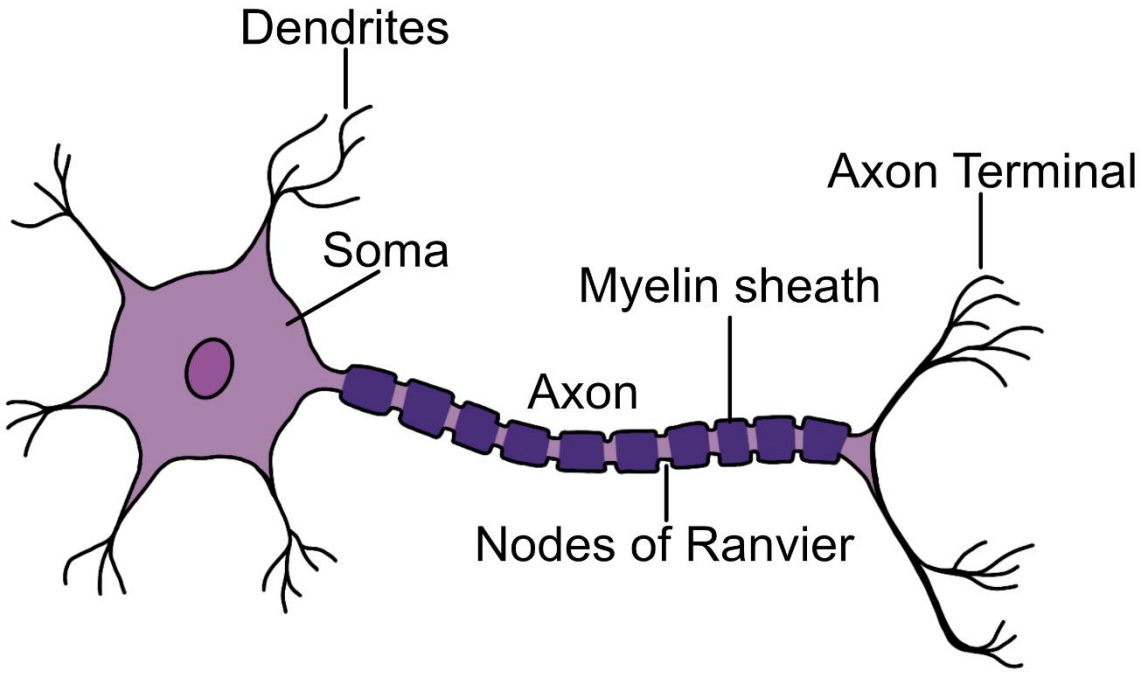

Figure 1 Functional units of the neuron. Dendrites are connected to other neurons and receive information, while the soma contains cell organelles. Information is transferred along the axon, which the myelin sheath insulates. Small gaps known as nodes of Ranvier are present between the sheath, where action potentials can form, enabling fast signal transfer. Ultimately, information is transmitted to other neurons via the axon terminal (adapted from Sadava et al., 2011).

The neuron has a semipermeable membrane, which is crucial for generating an electrical signal. Two selective ion channels along the membrane allow sodium or potassium to diffuse. Both are positively charged ions. They have different concentrations in the intracellular or extracellular milieu of the neuron. The concentration of potassium is higher in the extracellular milieu. For sodium, the concentration in the intracellular milieu is higher. The concentration of negatively charged ions makes the neuron's inner milieu more negatively charged than the extracellular milieu. At rest, the neuron is negatively charged at around -70 mV (Sadava et al., 2011). When the neuron is depolarised, the membrane potential becomes less negatively charged, voltage-dependent potassium channels open (see Figure 2), and potassium flows along its electrical and chemical gradient inside the cell, further depolarising it.

Voltage-dependent potassium channels open around -60 mV. A chain reaction occurs when the neuron reaches its threshold of around -50 mV, and more voltage-dependent potassium channels open. The neuron becomes positive (around 50 mV) for a few milliseconds (see Figure 2). Then voltage-dependent sodium channels open, and sodium flows out of the cell, repolarising the cell, meaning the cell becomes more negative again. Additionally, potassium channels close. Sodium channels do not close immediately; the cell becomes more negative than before for a few milliseconds; this is called hyperpolarisation (Sadava et al., 2011) (see Figure 2). The action potential is the short deflection of the membrane potential. The sodium-potassium pump, an enzyme, restores the membrane potential to its resting state. This active process of restoring the membrane potential consumes energy (Sadava et al., 2011). After an action potential, the neuron cannot produce another action potential for a short time period; we call this period the refractory period. This period is several milliseconds long (Sadava et al., 2011).

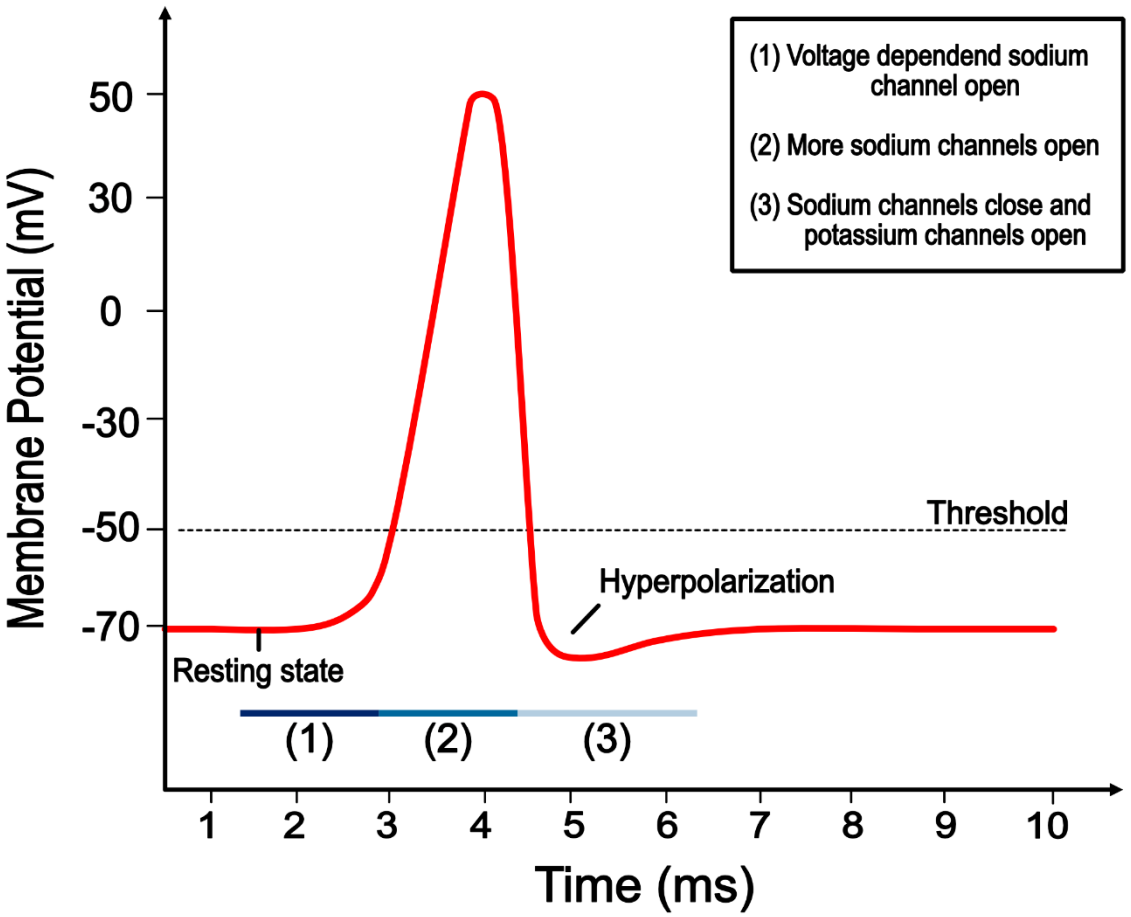

Figure 2 Action potential. The illustration depicts the process of generating an action potential. On the x-axis, time is measured in milliseconds, while the y-axis represents the membrane potential in millivolts. At rest, the membrane potential is approximately -70 mV. During depolarisation, voltage-dependent sodium channels open, allowing positive ions to enter the cell (1). Upon reaching a threshold of around -50 mV, additional sodium channels open (2), causing the cell to briefly become positively charged (approximately 50 mV). Subsequently, the sodium channels close, and potassium channels open (3), leading to the outflow of positive ions and causing the cell to become more negative for a brief period, a state known as hyperpolarisation. An active process then restores the cell to its resting state (adapted from Sadava et al., 2011).

There are different ways to transfer the signal from one neuron to another. The electrical signal is either transferred directly or indirectly using a chemical process. Gap junctions are tiny physical gaps between the neurons, which allow the transfer of electrical signals directly. The arrival of the action potential at the gap junction leads to a depolarisation of the adjacent neuron. This depolarisation is strong enough to produce a new action potential (Sadava et al., 2011). Chemical synapses transfer the electrical signal indirectly via chemical components called neurotransmitters. (Sadava et al., 2011). When the action potential reaches the axon terminal, it triggers a chemical process, releasing neurotransmitters. The neurotransmitters are stored and transported within the cell via vehicles.

These neurotransmitters diffuse to the next cell and bind to specific receptors (Figure 3 A). The neurotransmitter's receptors are ion channels, which can lead to depolarisation or hyperpolarisation. Depending on the type of receptor or neurotransmitter, the neuron is either hyperpolarised or depolarised (Sadava et al., 2011).

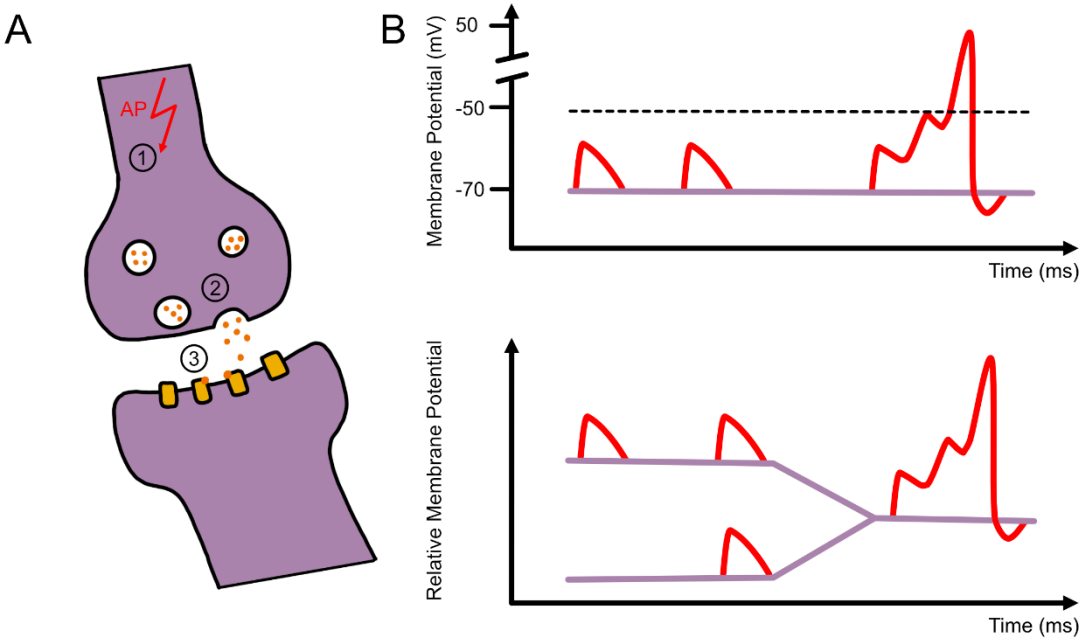

Figure 3 Synapse and postsynaptic potential. A) The figure depicts a synapse and the process of neurotransmitter release. Neurotransmitters, stored inside the cell, are released when an action potential (AP) arrives at the axon terminal (1). These neurotransmitters are then released (2), diffuse to the next cell and bind to receptors (3), which are ion channels. B) A schematic depiction of the postsynaptic potential. The upper figure illustrates the membrane potential in millivolts on the y-axis and time in milliseconds on the x-axis. It shows that when several excitatory postsynaptic potentials (EPSPs) arrive from the same synapse in close succession, they are linearly integrated and can lead to an action potential. The lower figure demonstrates a similar scenario for two dendrites, indicating that EPSPs can also be linearly integrated over space, leading to an action potential when arriving from two synapses simultaneously (adapted from Pinel et al., 2017; Sadava et al., 2011).

This deflection of the membrane potential is also called the postsynaptic potential (PSP) (Pinel et al., 2017; Spieler and Schumacher, 2019). The PSP can be positive or negative, depending on the influx or efflux of positively charged ions. Excitatory postsynaptic potentials (EPSP) increase the chance of an action potential by depolarising the cell. Inhibitory post-synaptic potentials (IPSP) decrease the chance of an action potential by hyperpolarising the cell (Buzsáki, 2006; Hansen et al., 2010; Schomer et al., 2018; Spieler and Schumacher, 2019). Notably, a single chemical synapse does not produce a strong enough PSP to trigger an action potential (Pinel et al., 2017) (Buzsáki, 2006). A single PSP has a smaller amplitude compared to an action potential.

Therefore, a single EPSP cannot reach the membrane potential threshold to trigger an action potential. However, they last longer compared to an action potential. Because they last longer, the neuron linearly integrates multiple PSP over time and space (see Figure 3 B). This means this summation of several EPSPs can lead to an action potential. On the other hand, ISPS can cancel the depolarisation of EPSP. While PSPs last longer than an action potential, their amplitude decreases over time and space. (Pinel et al., 2017). Therefore, several synapses must be active at the same time to generate an action potential.

Oscillations

Oscillations are a repeating variation over time (Buzsáki, 2006; Spieler and Schumacher, 2019); in the case of neuronal oscillations, they are the varying amplitude changes of brain activity. Their frequency, power and phase define them. The frequency is the number of cycles per time unit, expressed in Hertz (Hz). Power is the squared amplitude of the signal, and phase is the instantaneous phase angle value at a specific time, expressed in degree (Spieler and Schumacher, 2019). Neuronal oscillation can range between infra-low frequencies around 0.1 Hz or up to several hundreds of Hertz. They have been found in simple and more complex organisms (Spieler and Schumacher, 2019). In the case of the mammalian brain, oscillation can be found at the molecular, cellular, synaptic and network level (Spieler and Schumacher, 2019). Accordingly, they have been thoroughly investigated and are deemed an essential framework of information transmission within and between brain regions (Spieler and Schumacher, 2019).

The interplay between excitation and inhibition generates oscillations. Neuronal oscillations can be described as physical oscillators with a negative feedback loop. (Buzsáki, 2006). In a small local circuit, two neurons can produce an oscillatory behaviour. The local circuit needs an excitatory neuron, a neuron producing an EPSP and an inhibitory neuron, a neuron producing an IPSP. The excitatory neuron connects to other neurons and the inhibitory neuron. The inhibitory neuron connects back to the excitatory neuron (see Figure 4). The excitatory neuron receives excitatory input and produces an action potential. This activation leads to an activation of the inhibitory neuron (see Figure 4 A). The inhibitory neuron inhibits the excitatory neuron, which leads to a deactivation of the excitatory neuron (see Figure 4 B). Inhibition of the excitatory neuron deactivates the inhibitory neuron.

The inhibitory neuron stops producing action potential, meaning it stops inhibiting the excitatory neuron. This activates the excitatory neuron again (see Figure 4 C), and the loop starts from the beginning. (Buzsáki, 2006). This negative feedback loop demonstrates that inhibition is critical for generating oscillation. However, a single EPSP is not strong enough to produce an action potential. Therefore, several neurons must be synchronously excited (Hansen et al., 2010) as well as inhibited at the same time. So the activity pattern of several neurons is timed by inhibition (Buzsáki and Wang, 2012), which in turn produces fluctuating signals over time.

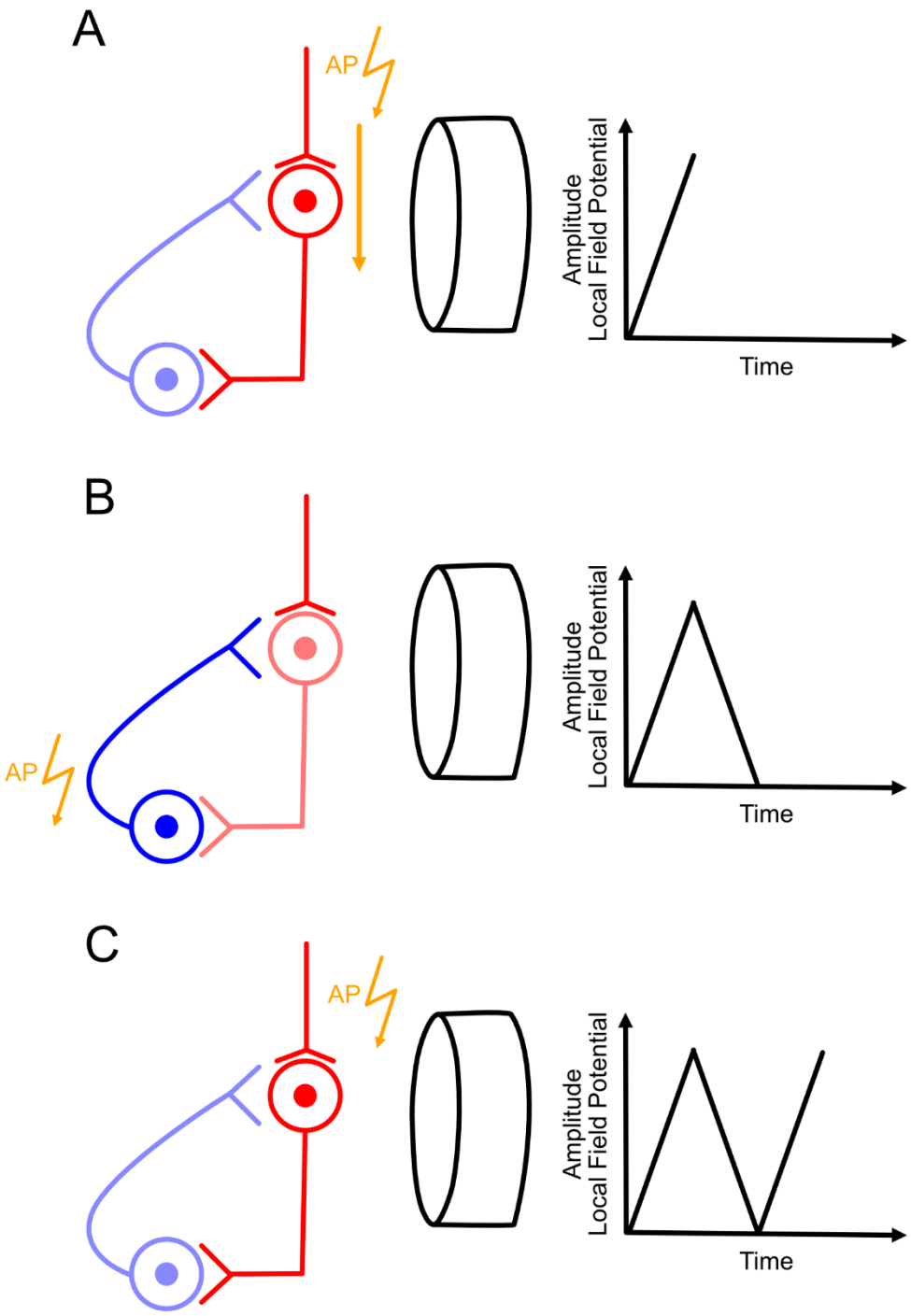

Figure 4 Oscillator. An excitatory neuron, shown in red, is connected to another excitatory neuron. The second excitatory neuron is connected to an inhibitory neuron, depicted in blue. The inhibitory neuron is connected back to the second excitatory neuron. An electrode (black oval) records the activity of the neurons. The left graph depicts a schematic of the activity (amplitude on the y-axis and time on the x-axis). The amplitude of the activity increases. A) The second excitatory neuron receives an action potential from the first neuron. This leads to the activation of the second excitatory neuron. B) Activating the second excitatory neuron leads to the activation of the inhibitory neuron. This inhibits the activation of the second excitatory neuron. The amplitude decreases. C) Due to the inhibition of the second excitatory neuron, the inhibitory neuron is not activated anymore, and cannot inhibit the second excitatory neuron. The amplitude of increases again (original work by Michelle Johannknecht, 2024).

Oscillations can have different frequencies. Different oscillators generate these frequencies in separate brain areas (Buzsáki, 2006; Schomer et al., 2018). The timing of inhibition, for example, how fast the synaptic transmission is between cell assemblies, is a defining factor in generating different frequencies (Buzsáki and Wang, 2012).

Classically, the frequency of oscillations is canonically restricted to different bands called delta, theta, alpha, beta and gamma (Schomer et al., 2018). Delta oscillations are wave-like shaped and with a frequency below 4 Hz. These slow oscillations are associated with physiological fluctuation, like blood-oxygenation level (Monto et al., 2008; Palva and Palva, 2012). Theta is defined between 4 and 7 Hz and stems from hippocampal networks. It is associated with spatial navigation and memory processes (Schomer et al., 2018). Alpha oscillations are between 8 and 12 Hz (Pinel et al., 2017) and can be found in the visual cortex, the somatosensory cortex (then called mu rhythm) and the temporal cortex (then called tau rhythm). Occipital alpha occurs during reduced visual attention and was previously believed to be an idling state of the brain, but nowadays, it is assumed that alpha functions as a gating mechanism for information by inhibiting the transmission of certain information (Buzsáki, 2006; Schomer et al., 2018). Beta (14 – 30 Hz) and higher frequencies are believed to be responsible for the spatial and temporal synchronisation of various cortical areas and for establishing global coherence between areas or networks (Schomer et al., 2018).

Oscillations can give us an insight into the temporal structure of the brain (Hari et al., 2010). They control neuronal activation or spike timing. So, single neurons adjust their firing pattern to the phase of the ongoing oscillation of the surrounding neuron population (Buzsáki, 2006; Spieler and Schumacher, 2019). Oscillations also facilitate interregional communication (Spieler and Schumacher, 2019), and they can represent hierarchical orders (Hari et al., 2010). Local processes are associated with faster oscillations compared to global processes, which are associated with slower oscillations (Hari et al., 2010).

Oscillations are helpful tools to investigate because they can control spike timing. We can view them as our brain's internal clock mechanism. They also seem to represent the hierarchical order of different brain regions.

Visual system

When light passes through the transparent media of our eye, it reaches the retina. (Pinel et al., 2017; Schomer et al., 2018). The retina is a complex component of the eye with different cell layers. One of the most essential cell types is the photoreceptor, a specialised neuron that reacts chemically to the appearance of light. They are responsible for translating the physical signal into an electrical signal.

The two photoreceptors on our retina are called rods and cones and differ in function and distribution on the retina (Pinel et al., 2017; Schomer et al., 2018). Rods are responsible for our ability to see in a dark or dimly lit environment. They are densely packed in the retina's periphery (Pinel et al., 2017; Schomer et al., 2018). Cones, on the other hand, are responsible for our ability to see colours. They are only active under bright conditions and are mainly located in the retina's centre. The visual accuracy is also higher for cones than for rods (Pinel et al., 2017; Schomer et al., 2018).

Both photoreceptors have in common the fact that light triggers a chemical reaction inside the cell, releasing neurotransmitters. These neurotransmitters produce an electrical signal in the ganglion cells (Pinel et al., 2017). Ganglion cells transmit information from our eye to the optic nerve, to the *lateral geniculate nucleus* (LGN) and from there to the primary visual cortex (Schomer et al., 2018).

Different cortical areas are involved in the processing of visual information. The primary visual cortex is located at the occipital cortex, but parts of the temporal and parietal cortex are also involved in processing visual information. The visual system is organised hierarchically. The information flow of the visual input is always from low-order information (like edges) to higher-order information (like the object's identity). Along the visual hierarchy, the receptive fields of neurons also change. The receptive field refers to the specific area of the visual field that neurons react to. In early visual areas, the receptive fields are small, meaning these neurons integrate only a small amount of information. In higher areas, the receptive field increases, allowing for the integration of more information. Therefore, the visual input information always goes from the retina to the primary visual cortex to the secondary visual cortex (Pinel et al., 2017; Sadava et al., 2011). However, two specialised pathways process specific information. They are the parvocellular and the magnocellular pathway.

Neurons of the parvocellular pathway react to detailed visual information like the object's colour, form and fine spatial details (Pinel et al., 2017; Schomer et al., 2018). The parvocellular pathway transfers information from the primary visual cortex to the secondary visual and then to the inferior temporal cortex. The magnocellular pathway transfers motion information and spatial information from the primary visual cortex to the secondary cortex in the parietal cortex (Pinel et al., 2017).

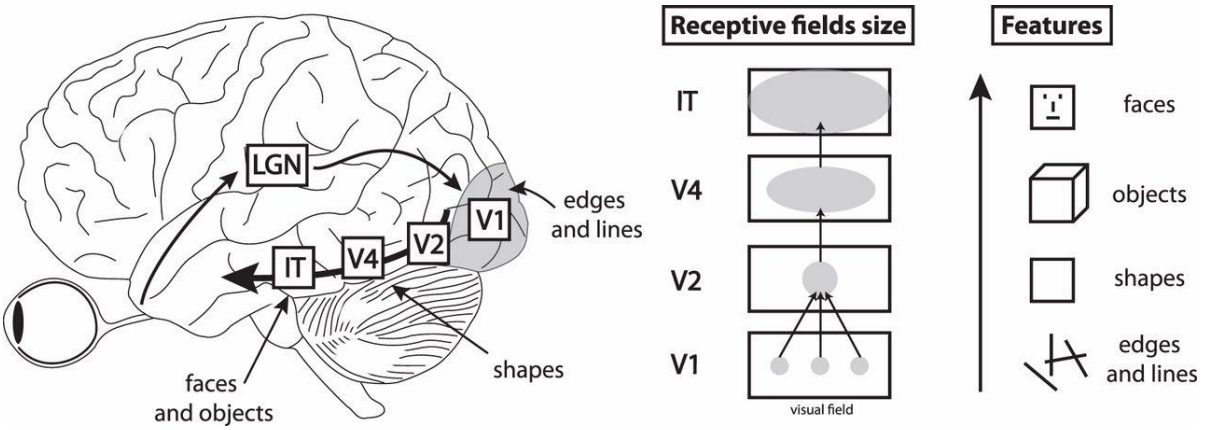

Figure 5 Visual Hierarchy. The diagram on the left depicts the flow of information through the visual hierarchy, starting from the eye to the lateral geniculate nucleus (LGN) and then on to the primary visual cortex (referred to as V1). The information is further processed in other areas of the visual system, flowing to the secondary visual area (V2) and then into higher areas of the visual system (depicted here V4 and the inferior temporal cortex (IT)). The middle illustration demonstrates that the receptive field of the neuron increases along the visual hierarchy, and that information is integrated along the way. On the right side, it is shown that the features processed along the hierarchy progress from simple features in early areas to complex features in higher areas (Manassi et al., 2013).

The two pathway hypotheses were established based on this separation of the information flow within the visual system and clinical observation. The parvocellular pathway processes information identifying objects and is called the "what pathway". Alternatively, it is also called the ventral stream because information flows along the ventral axis of the brain (Pinel et al., 2017). The magnocellular pathway transfers the information on the dorsal axis of the brain and is, therefore, called the dorsal stream. Because it processes spatial information of an object, it is also called the “where-pathway” (Pinel et al., 2017). An alternative hypothesis for the two-pathway-hypothesis is that these two pathways do not represent “what” and “where” more than the ventral pathways contain information for consciously identifying an object and the dorsal pathways contain information for spatially controlled behaviour (grabbing an object) (Pinel et al., 2017). However, these two pathways do not work independently (Pinel et al., 2017).

Additionally, to its hierarchal structure, the visual system is composed of modules. These modules are functionally specialised and process information locally (Schomer et al., 2018). Under these principles, we can conclude that early responses from our brain should happen from early activated areas of the visual hierarchy and that responses with longer latencies are from areas higher up in the hierarchical order (Hari et al., 2010).

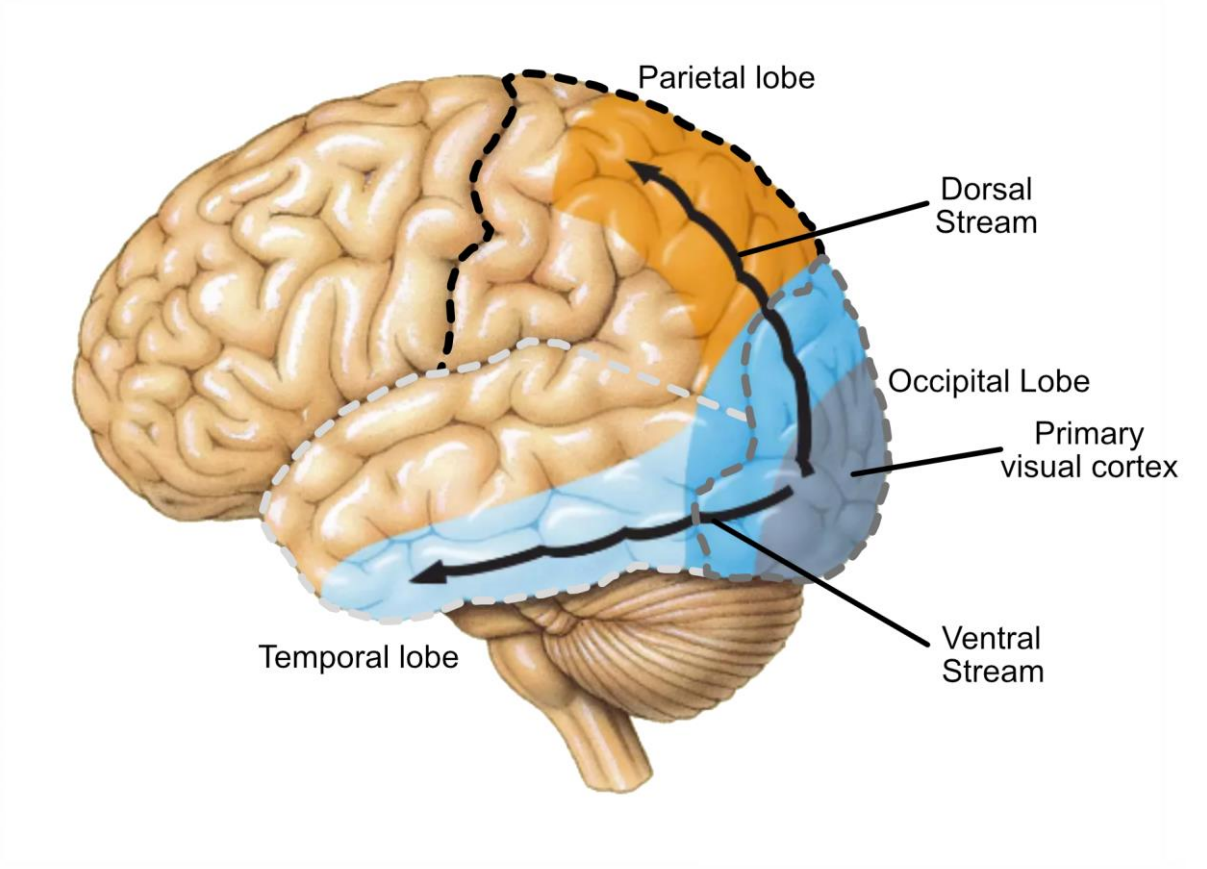

Figure 6 Two pathway hypothesis. The brain's visual processing involves two primary pathways: the dorsal and ventral streams. The dorsal stream originates from the primary visual cortex (blue-grey shaded area) and extends to the pre-striate cortex (mid-blue shaded area) and then to the posterior parietal cortex (orange shaded area). This pathway transfers information from the occipital lobe (dark grey dotted line) to the parietal lobe (black dotted line). The ventral stream also begins at the primary visual cortex, moves to the pre-striate cortex, and then to the inferotemporal cortex (light blue shaded area). Along this pathway, information flows from the occipital lobe to the temporal lobe (light grey dotted line) (adapted from Pinel et al., 2017).

Periodic perception

Oscillations are essential in vision; we assume they transfer information in chunks. The brain does not process all the visual information simultaneously (Buzsáki, 2006). Consequently, this assumes that our perception is periodic and not continuous. (VanRullen and Koch, 2003). Under continuous perception, we expect that perception does not change.

Therefore, all visual input is processed equally well; the neuronal signal strength should not change but be constant (VanRullen and Koch, 2003). Under a periodic process, we can assume that the neuronal signal strength fluctuates over time in the oscillation frequency responsible for the information transfer. In experimental settings using visual stimuli near the perceptual threshold, it has been shown that these visual stimuli are not constantly perceived but that the accuracy of perception changes over trials (VanRullen and Koch, 2003).

There are two main hypotheses about how oscillations drive our visual perception: that perception is a rhythmic or discrete process. Rhythmic perception assumes that the perception is better or worse depending on the momentary phase of the oscillations. In other terms, the likelihood of perceiving a stimulus depends on the phase of the underlying oscillation (see Figure 7 A and C) (VanRullen, 2016a). The idea of discrete perception is that the oscillation defines windows where perception is possible. This hypothesis focuses on the temporal scale of perception. When two identical stimuli fall within one perceptual window, we perceive them as a single event (see Figure 7 B and D) (VanRullen, 2016a).

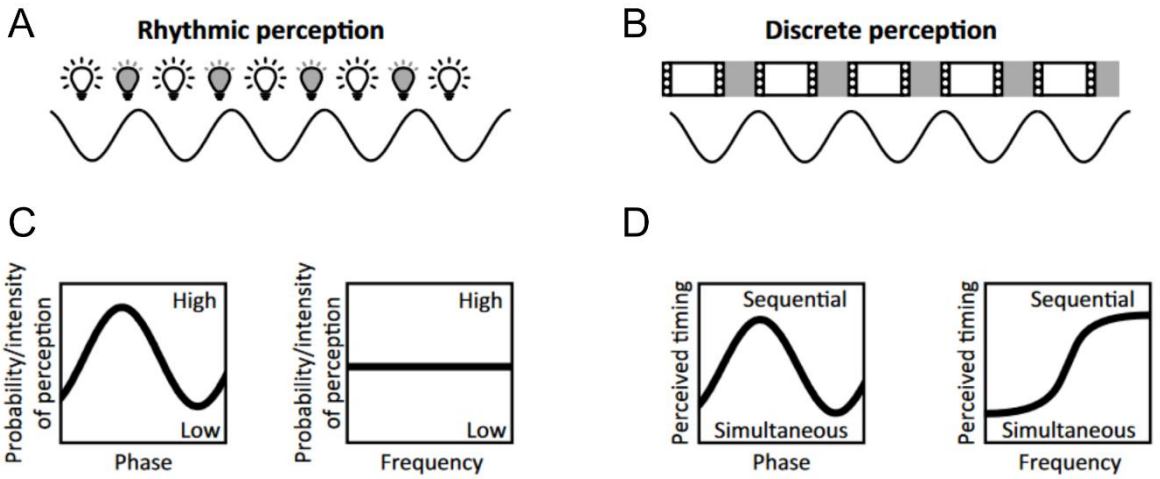

Figure 7 Periodic Perception. A) This illustrates the theory that our perception depends on the phase. The light lightbulbs represent good perception and the grey lightbulbs less good perception. B) This is an illustration of discrete perception. The oscillation determines windows of integration. During these windows, shown as film snapshots, visual stimuli are integrated over time. C) A formal description of A): Our probability of perception (y-axis on both sides) depends on the phase of the oscillation (x-axis on the left) but not on the frequency of the oscillation (x-axis on the right). D) A formal description of B): The perceived timing of two stimuli (y-axis on both sides) varies with the phase of the oscillation (x-axis on the left) and with its frequency (x-axis on the right), with higher frequency making it more likely to perceive both stimuli as sequential (VanRullen, 2016a).

There is evidence for both hypotheses in the literature. Oscillatory power, prior to the presented stimulus, has been correlated with the likelihood of detecting a near-threshold stimulus (Benwell et al., 2022; Iemi et al., 2017; Lange et al., 2013; Limbach and Corballis, 2016; van Dijk et al., 2008). Similarly, in the tactile domain, it was also shown, that oscillatory power correlated with the perception of simultaneously of two tactile stimuli (Baumgarten et al., 2016). Also, the prestimulus phase was correlated with the likelihood of perceiving a near-threshold stimulus (Busch et al., 2009; Busch and VanRullen, 2010; Dugue et al., 2011; Landau and Fries, 2012a; Mathewson et al., 2009; Milton and Pleydell-Pearce, 2016). Therefore, perception fluctuates over time depending on the momentary power or phase, indicating a rhythmic process.

However, studies also found evidence for discrete perception. These studies investigated the temporal scale of perception by varying the time between two identical stimuli and recording when participants integrated them into a single event. These studies investigated the peak frequency of an oscillation (the frequency with the highest oscillatory power), as a measure of the temporal resolution of our brain. Faster oscillation should create short integration windows, resulting in a higher temporal resolution. There is evidence that the peak frequency of the observer correlates with their temporal perception in unimodal (Samaha and Postle, 2015; Tarasi and Romei, 2023) but also multimodal tasks (Cecere et al., 2015; Migliorati et al., 2020). For temporal perception in the tactile domain, there is also evidence that the phase prior to the arrival of both stimuli correlates with perception and defines the temporal window of perception (Baumgarten et al., 2016).

Regardless of the underlying visual mechanism, alpha oscillation plays an important role. Most previous studies assumed a functional role of alpha oscillation for our perception. The challenge is to disentangle the underlying mechanism for visual perception because there is no consensus in the scientific community, and null findings have also been reported in recent years (Keitel et al., 2022).

Periodic Behaviour

Another indication that our perception is periodic would be that behavioural responses, relying on perception, should also be periodic. In visual tasks, we can see that also behaviour is periodic. However, this periodicity shows when an additional stimulus was shown before the actual task. This stimulus is usually above the perceptual threshold and task-irrelevant.

Commonly, the experimenter shows the task-irrelevant stimulus prior to the task stimulus, with varying time delays between these two. The behavioural response is then reconstructed as a function of the time delay between task-irrelevant stimulus and task stimulus. (Landau and Fries, 2012a; Plöchl et al., 2022; Tosato et al., 2022). In these tasks, the behavioural response often fluctuates around 4 to 7 Hz. However, the problem with these tasks is that the external stimuli can capture attention, which can then module the underlying oscillation (Mudrik and Deouell, 2022).

Research suggests that external stimuli can reset the ongoing neuronal oscillation. (Buzsáki, 2006). The external stimuli disrupts the ongoing oscillation and resets it to a uniform phase value. As a result, the neuronal oscillation is phase-aligned after the stimulus (Ferrè et al., 2016; Fiebelkorn et al., 2011; Gruber, 2005; Makeig et al., 2002). In experiments where a task-irrelevant stimulus is shown prior to the task stimulus, it is assumed that this stimulus produces a phase reset. Additionally, the timing between task-irrelevant stimulus and task stimulus is varied systematically. Therefore, the underlying oscillation is also modulated systematically by inducing a phase reset at different time delays. This systematic phase reset then leads to behavioural fluctuation because the phase is aligned prior to the presentation of the task stimulus. When the behaviour is then a function of the phase of the underlying oscillation, this enhances the relationship between the oscillatory phase and behaviour, leading to the observed behavioural fluctuations. In the context of periodic perception, this would mean that either the phase of the oscillation is systematically shifted or the window of integration. As mentioned before, alpha oscillation seems to be relevant for visual perception. However, the results for periodic behaviour show that behaviour fluctuates between 4 to 7 Hz. This discrepancy could be explained by the above threshold stimulus capturing the observer's attention and modulating another attention-related mechanism, not a perception-related one.

Alternatively, the task-irrelevant stimulus could be subliminal instead of above the threshold. Subliminal stimuli are weak stimuli and are not consciously perceived by the observer (Dehaene et al., 2006). These subliminal stimuli can modulate behavioural responses (Bareither et al., 2014; Baumgarten et al., 2017a; Ferrè et al., 2016; Mudrik and Deouell, 2022) and also elicit brain responses which are distinct to responses for above-threshold stimuli (Iliopoulos et al., 2020; Railo et al., 2021; Silverstein et al., 2015).

In summary, there is a distinction between rhythmic and discrete perception. Rhythmic perception assumes that perception is a function of the phase of the neuronal oscillation. Discrete perception assumes that the neuronal oscillation defines temporal windows of integration. In the literature, there is evidence for both hypotheses. In a visual experiment using additional stimuli before the task stimulus, the behaviour fluctuated as a function of the time delay between the task-irrelevant stimulus and the task stimulus. Subliminal stimuli could be an alternative for using above-threshold stimuli to evoke rhythmic behavioural responses.

MEG

The MEG measures the magnetic field outside the scull, which is produced by the biochemical processes (Hämäläinen et al., 1993; Hillebrand & Barnes, 2002; Lopes da Silva, 2013; Pinel et al., 2017) of a large number of interacting neurons (Buzsáki, 2006). The recording method is reference-free and non-invasive (Baillet et al., 2001; Hämäläinen et al., 1993; Hari et al., 2010; Uhlhaas et al., 2017, 2017). The signal the MEG capture contains several frequencies, ranging between <1 Hz up to several 100 Hz (Schomer et al., 2018). The MEG has a spatial precision of a few millimetres (Buzsáki et al., 2012; Hämäläinen et al., 1993; Schomer et al., 2018) and a temporal resolution in the millisecond range (Baillet et al., 2001; Hämäläinen et al., 1993; Hari et al., 2010; Uhlhaas et al., 2017).

A fundamental assumption of the MEG is that the neuron functions as a current dipole. A current dipole is formed when two charges of opposite polarities are separated by some distance (Buzsáki, 2006). When positively charged ions enter the neuron due to an EPSP, the area inside the neuron near the excitatory synapse becomes more positively charged. We call this area the source. In comparison, areas inside the neuron, further away from the synapse, are more negatively charged. We call this the sink. Ions flow from the sink to the source (Buzsáki et al., 2012). This current flow inside the neuron is also called the primary current (Baillet et al., 2001), the primary source of the MEG signal (Buzsáki et al., 2012; Hansen et al., 2010). There is also a returning or secondary current occurring outside the neuron. After an EPSP, the outside of the synapse is more negatively charged than areas further away from the synapse—the secondary current flows opposite to the primary current (Buzsáki et al., 2012).

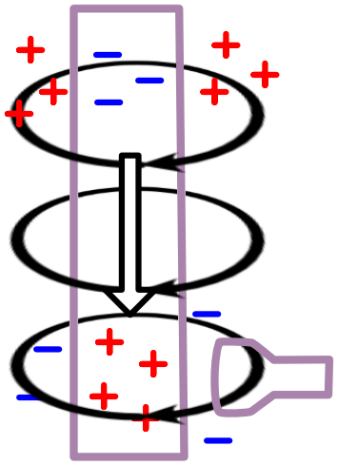

Figure 8 Current Dipole. The illustration shows the formation of a current dipole inside a stylised axon (purple column). Around the excitatory synapse on the bottom, positively charged ions enter the cell. The area further away from the synapse is more negatively charged. The current flow, depicted as the arrow, goes from the negative sink to the positive source. The primary current inside the cell is shown (original work by Michelle Johannknecht, 2024).

This current flow of the dipole generates electrical and magnetic fields. The magnetic field is orthogonal to the electric field (Spieler and Schumacher, 2019). However, a single dipole is not strong enough to create a measurable signal outside the scull. Therefore, several neurons must be active at the same time. The dipoles must have the same orientation for superimposing these magnetic fields. Therefore, we measure the weighted sum of parallel active currents (Baillet et al., 2001; Vrba and Robinson, 2001) (Schomer et al., 2018). The dipoles are weighted based on a few factors: their orientation to the surface (perpendicular dipoles are the best source for the MEG signal) (Baillet et al., 2001; Vrba and Robinson, 2001), the density of the active neurons, the temporal correlation between them and the distance to the sensor (Hari et al., 2010; Schomer et al., 2018). We call this summed activity of the dipoles the local field potential (LFP). Synaptic activity is the main generator of the LFP, but there are also non-synaptic events (like action potentials) that contribute to the strength of the LFP (Buzsáki, 2006; Buzsáki et al., 2012; Hari et al., 2010). Cortical pyramid cells are a good candidate for generating strong LFPs. They are geometrically aligned and are tangential to the skull (Hansen et al., 2010; Hari et al., 2010; Schomer et al., 2018; Spieler and Schumacher, 2019).

We use Maxwell's equations to describe the strength and spread of the magnetic field of the pyramid cells. The equations assume that we know the source of the magnetic field (Baillet et al., 2001; Hämäläinen et al., 1993). For simplification, it is often assumed that the head is a sphere and a homogeneous conductive medium (Hämäläinen et al., 1993; Hansen et al., 2010).

Our brain produces a weak magnetic field (around 0.1 μT) compared to the earth's magnetic field (between 22 and 67 μT). Sensors capturing this small magnetic field are called superconducting quantum interference devices (SQUID) (Hämäläinen et al., 1993; Pinel et al., 2017).

A SQUID is a superconducting ring interrupted by two Josephson junctions and works on the quantum interference principle (Hämäläinen et al., 1993). A SQUID translates small fluctuations of an applied magnetic field into recordable electrical voltage changes (Hari et al., 2010). To function, SQUIDs have to reach their superconductive state, meaning that they have zero electrical resistance (no energy lost due to heat) (Clarke, 1994; Hämäläinen et al., 1993). They are cooled down with liquid helium to around -270°C to reach their superconducting state (Buzsáki, 2006).

Within this state, the so-called Cooper Pairs form. Cooper Pairs are two electrodes that attract each other instead of repelling each other, as they would normally. These pairs move through the lattice of the superconducting material, leaving a negatively charged surrounding behind them. This movement resembles a ripple or a wave (Clarke, 1994; Hämäläinen et al., 1993).

A Josephson junction is a bridge within the superconducting material. It is characterised by a critical current that can pass through it (Clarke, 1994; Hämäläinen et al., 1993). Cooper pairs can pass the bridge and, along their movement, generate waves. We refer to this wave-like behaviour as quantum interference. A valid quantum interference happens when the wave generated by Cooper Pairs is in phase at both Josephson Junctions (Clarke, 1994; Hämäläinen et al., 1993).

We apply a current to the superconductive ring to measure any change in a small magnetic field. This current leads to the formation of Cooper Pairs, which then move over the Josephson junctions. This movement creates then a valid quantum interference (see figure 9 A). When we expose the SQUID to a magnetic field, this magnetic field alters the phase of the waves created by the Cooper Pairs at the two Josephson junctions. These phase changes affect the critical current that can pass through the Josephson junctions (see figure 9 B).

We then measure the voltage across the SQUID, which swings back and forth, according to the change in the magnetic field applied to the SQUID (Clarke, 1994; Hämäläinen et al., 1993).

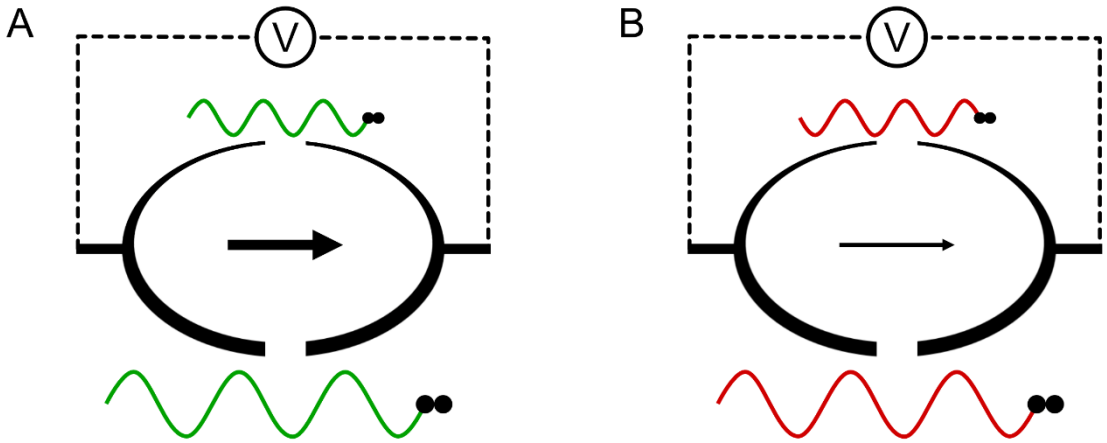

Figure 9 Magnetic field measurement. The schematic shows how a small magnetic field is measured using a SQUID. The SQUID ring is depicted as the black ring. The Josephson junctions are the gaps in the ring. The critical current that can flow through the Josephson junction is depicted as the arrow in the middle of the ring. A current is applied to the ring. To measure changes in the magnetic field the voltage across the ring is measured. A) Here a valid quantum interference is measured. Indicated by the phase-aligned wave-like behaviour of the Cooper Pairs (black dots) at both Josephson junctions. The current can flow according to the critical current of the Josephson junctions. B) An invalid quantum interference happens after the SQUID is exposed to a magnetic field. The critical current changes and the voltage we measure across the SQUID changes accordingly. The magnetic field is not shown (original work by Michelle Johannknecht, 2024).

Because SQUIDs are sensitive to tiny magnetic fields, we apply several techniques to reduce the noise of other magnetic fields. One hardware solution is the use of flux transformers. Flux transformers are coils connected to the SQUID. They work as a filter for the magnetic field. This means they emphasise small changes in the brain's magnetic field and attenuate other magnetic sources (Hari et al., 2010; Schomer et al., 2018). To reduce further external noise, like power line noise, the measurement takes place in a magnetically shielded room constructed of mu-metal and aluminium (Hari et al., 2010; Schomer et al., 2018).

To summarise, the MEG can record the brain's magnetic field with high precision using highly sensitive SQUIDs. These devices rely on quantum physical principles and are sensitive enough to detect small changes in a weak magnetic field. The recording takes place in a magnetically shielded room to ensure data quality and special hardware is installed in the MEG to reduce the noise.

Inverse Problem

As mentioned before, Maxwell's equation solves the forward problem, which is how the magnetic field spreads when the source of the magnetic field is known (Baillet et al., 2001). The MEG records the magnetic field, but the source of the field is unknown. This is known as the inverse problem. Specifically, the inverse problem refers to the mathematical problem that we cannot unambiguously compute the source of the measured signal at the scull (Buzsáki et al., 2012). Knowing the origin of the source inside the brain can help us understand which brain areas are active during a specific process. The inverse problem is challenging because there is no single solution (Baillet et al., 2001; Hansen et al., 2010). Therefore, constraints must be applied to find the best solution to explain the measured signal (Hari et al., 2010).

Individual magnetic resonance images (MRI) of the subject's brain help to improve source estimation. The brain images are aligned with the recorded data (Baillet et al., 2001). The use of head models improves the spatial accuracy of our estimation. One method to estimate the source is the linear constrained minimum variance beamformer (LCMV beamformer). The goal of this method is to minimise the variance of the output we get from the model. In this case, the output is the power spread of a specific source. The model works as a spatial filter; the current source should be highlighted while surrounding sources are attenuated (Baillet et al., 2001). The constraints of the LCMV beamformer are that much data is necessary to estimate so-called virtual channels or small linear integrated sources. Therefore, non-averaged and ongoing data is used to create this model (Hansen et al., 2010).

Objectives of this thesis

In this thesis, I investigated the relationship between neuronal oscillations in the alpha range and the ability to integrate two visual images temporally. The aim was to disentangle whether temporal visual perception is a rhythmic or discrete process.

In the first study, I investigated the relationship between neuronal oscillations prior to the used test stimulus and our ability to integrate two complementary visual stimuli temporally. I recorded the brain activity using MEG and correlated features of the prestimulus oscillation (phase and frequency) with the observer's behavioural results (accuracy).

I hypothesised that the prestimulus alpha phase modulates behaviour and not frequency. I expected behavioural response (correct vs incorrect) to be at opposite phases and that the perceptual integration window would not correlate with frequency. I conducted the second study based on the first study's results, further extending the understanding of temporal visual perception. I used the same visual integration task but modified the prestimulus period by presenting a subliminal visual stimulus to the observer. We correlated the observer's behavioural response with the delay between the test stimulus (visual integration task) and the subliminal stimuli. I hypothesised that the subliminal stimulus would lead to behavioural fluctuations. I expected behavioural fluctuations in the 8 to 12 Hz range.

Study One: Prestimulus alpha phase modulates visual temporal integration

Contributions

Michelle Johannknecht: Performed research, analysed the data and wrote the manuscript

Prof. Dr. Alfons Schnitzler: Wrote the manuscript

PD Dr. Joachim Lange: Conceptualized research, analysed the data and wrote the manuscript

Published 12th August 2024 in eNeuro; DOI: https://doi.org/10.1523/ENEURO.0471-23.2024

Abstract

When presented shortly after another, discrete pictures are naturally perceived as continuous. The neuronal mechanism underlying such continuous or discrete perception are not well understood. While continuous alpha oscillations are a candidate for orchestrating such neuronal mechanisms, recent evidence is mixed. In this study, we investigated the influence of prestimulus alpha oscillation on visual temporal perception. Specifically, we were interested whether prestimulus alpha phase modulates neuronal and perceptual processes underlying discrete or continuous perception. Participant had to report the location of a missing object in a visual temporal integration task, while simultaneously MEG data was recorded. Using source reconstruction, we evaluated local phase effects by contrasting phase angle values between correctly and incorrectly integrated trials.

Our results show a phase opposition cluster between - 0.8 to - 0.5 s (relative to stimulus presentation) and between 6 - 20 Hz. These momentary phase angle values were correlated with behavioural performance and event related potential amplitude. There was no evidence that frequency defined a window of temporal integration.

Introduction

Although our everyday experience implies that perception is a seamless process, the human perceptual system is limited to accurately detect and process incoming information. These limitations affect e.g., the spatial but also the temporal resolution of perception. For example, a series of discrete stimuli will be perceived as a continuous, seamless flow of information, if the presentation duration is faster than the temporal resolution of the visual system – like in movies.

Research in the last decades has highlighted a functional role of neuronal oscillations for perception. Especially prestimulus alpha oscillations have been shown to be a relevant factor for perception near threshold. For example, recent studies demonstrated, the power of alpha oscillations influences perception in near-threshold detection tasks (Baumgarten et al., 2016; Benwell et al., 2022; Iemi et al., 2017; Lange et al., 2013; Limbach and Corballis, 2016; van Dijk et al., 2008).

In addition, evidence showed that the momentary phase of prestimulus oscillations influences the detectability of stimuli in near-threshold detection task (Busch et al., 2009; Busch and VanRullen, 2010; Dugue et al., 2011; Landau and Fries, 2012b; Mathewson et al., 2009). While most of the evidence for a potential role of phase for perception stems from detection tasks, few studies also reported an influence of phase on temporal perception (Baumgarten et al., 2015; Ikumi et al., 2019; Milton and Pleydell-Pearce, 2016).

Despite the accumulating evidence for a functional role of alpha phase for visual perception, there are still unresolved questions and remaining concerns. For instant, while some studies reported an influence of alpha phase on perception, other studies reported null results (summarized by Keitel et al., 2022). Moreover, inconsistencies in the reported frequency ranges in similar tasks raise the question of validity of these findings (Merholz et al., 2022). Finally, the functional role of prestimulus phase remains unclear. Prestimulus phase might modulate sensory processing by modulating poststimulus evoked potentials (Busch and VanRullen, 2010; Milton and Pleydell-Pearce, 2016).

Other studies propose that the phase effects may indicate that specific frequency bands are relevant for perceptual integration or segregation of uni- or multimodal stimuli (Baumgarten et al., 2015; Ikumi et al., 2019; Wutz et al., 2018).

While most studies focused on the role of phase for detection, few studies investigated the role of phase for temporal integration of visual stimuli. Wutz et al. (2016) used the same task as we used in the present study to investigate visual temporal integration or segregation, with as strong focus on the neural activity in the theta-band. They reported phase differences in the theta-band depending on the task (integration or segregation) and participants' response (correct or incorrect; Wutz et al., 2016). In a follow-up study, the authors focused on the functional role of frequency for visual integration and segregation (Wutz et al., 2018). In addition, Milton & Pleydell-Pearce (2016) found that prestimulus phase correlated with performance in a temporal simultaneity task. In the present study, we expand these finding by determining whether the prestimulus phase influences temporal integration mechanisms by modulating early poststimulus sensory processing or whether the frequency of prestimulus phase effects determines temporal integration windows. We want to deepen the understanding of the neural mechanisms of temporal integration by looking into the momentary prestimulus phase in a broad spectrum of frequencies. First, we want to investigate how the prestimulus phase influences behavioral performance. Further, in addition to most other studies, we want to investigate whether putative prestimulus phase effects mediate poststimulus neural processing or whether prestimulus phase effects support the hypothesis of temporal windows of integration. To investigate these hypotheses, participants performed a visual temporal integration study (Wutz et al., 2016), while we simultaneously recorded their neural activity using MEG. We analysed whether the phase of neuronal oscillations correlated with successful integration of the visual stimuli and poststimulus sensory processing.

Materials and Methods

Participant and ethical information

We recruited 25 participants (17 female, mean age 25.4 ± 5.1 years [SD]) for this study. We chose the number of participants based on previous paper using the same task (Wutz et al., 2018, 2016). The participants provided written informed consent in line with the Declaration of Helsinki and the Ethical Committee of the Medical Faculty, Heinrich Heine University, approved the study. No participant reported to have any neurological or psychological disorder. All participants had normal or corrected-to-normal vision. Participants received 10€ per hour for participation.

Stimuli and Task

We adapted the stimuli and task design from Wutz et al. (2016). Each trial started with a randomized prestimulus period between 1200 – 1600 ms with a central fixation cross, followed by the presentation of the stimulus (Fig. 10). A stimulus consisted of two images presented for 16 ms, each. Both images were separated by individual stimulus onset asynchronies (SOAs, see below for details on the SOA). Each image showed seven full annuli and one-half of an annulus presented on pseudo-random positions on a 4 x 4 grid. When both images are integrated, annuli fill out each position, except one. A post-stimulus period followed the stimuli, with a random duration between 600 – 1200 ms with only a fixation cross. Finally, an instruction text appeared which prompted participants' responses. Participants' task was to report the empty position. Importantly, participants could report the position only if they temporally integrated both images. Participants reported the position of the missing element by responding twice: The first response was to report the number of the row of the missing element and the second response to report the column number within the 4x4 grid. Participants responded with their right hand via button press. When they responded too early (before presentation of the instructions) or too late (>2000 ms after presentation of instructions), they received feedback accordingly and the trials was appended to the end of the block.

We projected the stimuli on a translucence screen using a projector located outside the magnetically shielded room (Panasonic, PT-DW700E; 60 Hz refresh rate) and a mirror system. The screen was 140 cm away from the participant.

Grid dimensions were 8 x 8 cm (i.e., visual angle of 3.5° x 3.5°, each annuli was 1 x 1 cm in size; annuli were evenly spaced on the grid). A training session of ~2-5 min preceded the experiment.

Before the main experiment, we used a staircase method to measure the performance threshold of 50 % performance accuracy. The staircase started with a fixed SOA of 26 ms. The SOA increased when participants answered twice in a row correct or decreased when they answered twice incorrect. The step size of the increase/decrease was 16 ms (e.g. one frame). When performance was stable at 50% accuracy over the last 20 trials (i.e., the variance of SOAs was < .5), the staircase terminated and the current SOA was taken as the threshold SOA. The staircase was interleaved with SOAs randomly picked from the predefined SOA distribution (starting at 0 ms and increased in steps of 16 ms up to 144 ms). These random SOAs were not included in the computation of the threshold SOA. The threshold SOA is the temporal offset between the two images the participant needed to integrate both images in 50 % of trials. We used additional SOA conditions (0 ms [i.e., both images presented directly after each other], threshold SOA ± 16 ms, threshold SOA + 48 ms) to monitor participants' behaviour (Baumgarten et al., 2017b, 2015). One block consisted of two repetitions of the long (threshold SOA ± 48 ms) and short SOA (0 ms) each, four repetitions for each of the intermediate conditions, and 15 repetitions of the threshold SOA, all stimuli presented in pseudo-randomized order. The entire experiment consisted of 15 blocks and lasted between 30 min and 45 min. After every 100 trials, the participant could take a self-paced break. We used the software Presentation (Neurobehavioral System, Albany NY, USA) to control the experiment.

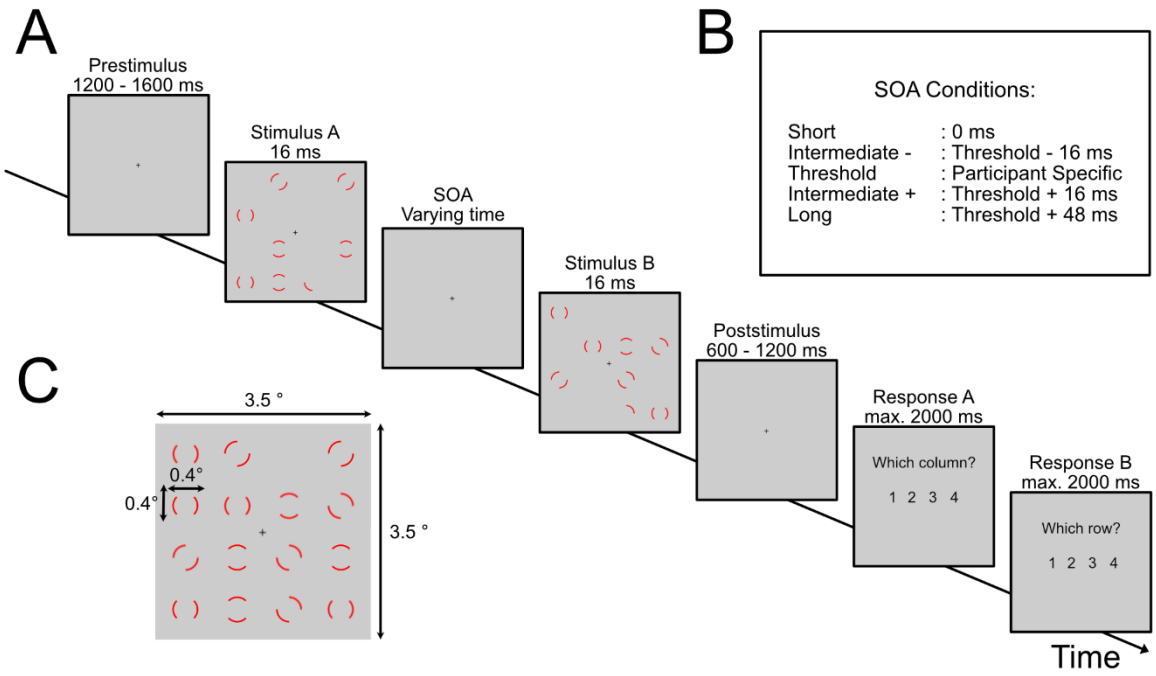

Figure 10 Paradigm study one. (A) The experiment started with a prestimulus phase (randomly between 1200-1600 ms) where only a fixation cross was presented. Afterwards the first stimulus was presented for 16 ms, followed by a stimulus offset asynchrony (SOA) and the second stimulus. After a poststimulus period (randomly between 600-1200 ms), participants reported the position of the empty location. (B) The different SOA conditions used in the experiment. The threshold SOA was individually determined to achieve 50 % accuracy. (C) An example of a full integration of the two stimuli.

MEG recording

During the experiment, we recorded the electromagnetic signal of the brain using a 306-channel Magnetoencephalography (MEG) system (MEGIN, Finland), with a sampling rate of 1000 Hz. The electrooculogram (EOG) was simultaneously recorded by placing electrodes above, below the left eye, and on the right and left temple. The head position inside the MEG was co-registered using four head position indicator (HPI) coils. We placed the coils behind the left and right ear and on the right and left forehead. We digitized the coil positions, anatomical landmarks (nasion, left and right periauricular points) and ~50-100 additional points from the head using the Polhemus digitizer (Fastrak, Polhemus, Vermont, USA).

MRI recording

For each subject, we recorded a structural magnetic resonance image, with a 3-T MRI scanner (Siemens, Erlangen, Germany). Afterwards, MEG data was aligned offline with the MRI using anatomical landmarks (nasion, left and right pre-auricular points).

Behavioural analysis

We analysed the behavioural data on group level by calculating the fractional accuracy for each SOA condition and subject. We averaged the individual fractional accuracies across participants. To test for statistical difference in accuracy per SOA, we performed a one-way ANOVA and post hoc Tukey-Kramer tests for pairwise comparisons between SOAs. See also table S1 for an overview of the statistical tests performed.

Preprocessing of MEG data

For the analysis of MEG data, we used MATLAB (R2019b) and the analysis toolbox FieldTrip (Version 20210825; Oostenveld et al., 2011). First, we divided the continuous MEG data into trials starting with the presentation of the fixation cross and ending with the presentation of the response instructions. We removed jump artefacts, eye movement and muscle movement, using a semi-automatic approach implemented in FieldTrip. We applied band-stop filters between 49 Hz to 51 Hz, 99 Hz to 101 Hz and 149 Hz to 151 Hz, to remove power line and a band-pass filter between 2 and 200 Hz to the data. Next, we visually inspected the data to remove noisy channels and trials. Finally, we used independent component analysis (ICA) to remove undetected noise or artefacts. To speed up ICA, we resampled the data to 150 Hz.

Source projection of MEG data

Source grid models were computed by applying a regular spaced 3D grid with 5 mm resolution to the Montreal Neurological Institute (MNI) template brain provided by the FieldTrip toolbox in MATLAB (R2019b). We computed individual grids by nonlinearly warping the individual structural MRI on the MNI MRI, after which we applied the inverse of this warp to the MNI template grid, which resulted in the individual warped virtual sensor grid.

Next, we calculated spatial filters in the time domain by computing a lead field matrix for the reconstructed warped visual sensor grid (Nolte 2003), and using data between -1 s and -0.5 s. We calculated spatial filters using the linear constrained minimum variance beamforming approach (Van Veen 1997) and projected the sensor time-series MEG data through these filters. This projection resulted in time-series data for each grid point. We restricted from here further analyses to regions of interest (ROI), defined by the AAL atlas (Tzourio-Mazoyer et al., 2002) implemented in FieldTrip. We expected to see effects in early visual areas and thus restricted the ROI to these areas.

We included the following regions (left and right hemisphere): *Calcarine fissure, Precuneus, Lingual gyrus, Cuneus, Superior occipital lobe, Middle occipital lobe, Inferior occipital lobe, Suberior parietal gyrus, Inferior parietal gyrus*.

Calculating phase opposition sum and surrogate data

To analyse whether the phase of neuronal oscillations influences temporal integration, we included only threshold SOA trials. We sorted the trials into three different groups: "correct" (including only trials where the coordinates of the missing element were correctly reported), "incorrect" (trials where the coordinates were not correctly reported), and the combination of correct and incorrect, which will be labelled "all".

We analysed phase differences between correct and incorrect trials using the phase opposite sum (POS, VanRullen, 2016). To this end, we calculated for each grid point and trial a Fast Fourier Transformation (FFT) for frequencies between 2 Hz to 30 Hz in steps of 2 Hz. The time window of interest was the prestimulus period between -1 s to 0 s (onset of stimulus). We used a sliding window of 0.3 s length, moved in steps of 0.05 s. Prior to FFT, we multiplied the data with a single Hanning taper. Next, we calculated for each condition the inter trial coherence (ITC), which is a measure for phase consistency across trials (VanRullen, 2016b).

$$ITC_{all} = \left|\sum_{[i = 1{:}n]} \omega_i/|\omega_i|\right| /n$$
$$ITC_{correct} = \left|\sum_{[i \in n_{correct}]} \omega_i/|\omega_i|\right| /n_{correct}$$
$$ITC_{incorrect} = \left|\sum_{[i \in n_{incorrect}]} \omega_i/|\omega_i|\right| /n_{incorrect} \quad (1)$$

N refers to the number of trials in each group and ω to the angle at trial i.

Using the ITC values, we calculated the phase opposition sum (POS).

$$POS = ITC_{correct} + ITC_{icorrect} - 2ITC_{all} \quad (2)$$

The POS value was calculated for each time-frequency-grid point sample independently. POS values are bound between zero and two, zero indicating that the phase values between correct and incorrect are identical and positive values indicate that phase values are different between correct and incorrect. Since trial number biases ITC, we picked randomly a subset of trials from the group with the higher trial count to equal the number of trials with the group containing fewer trials and then computed ITC and POS values. The average trial number for correct trials was 87.4 (± 34.4 STD) and for the incorrect trials 81.2 (± 25.1 STD). We repeated this step 100 times, resulting in 100 POS values per time-frequency-grid point sample. We calculated the median of POS values per subject and time-frequency-grid point sample.

These observed POS values were statistically tested against a null distribution of surrogate data. We created surrogate data by shuffling the trials from group correct and incorrect, while accounting for equal trial count. We selected 100 times randomly trials and calculated the mean POS values. POS values were calculated as described above. We calculated for each participant 100 mean POS values for each time-frequency-grid point.

To test for group level effects of the POS effect, we used a cluster-based permutation approach (Oostenveld et al., 2011). We first normalized the individual POS values by subtracting the mean and dividing by the standard deviation of the surrogate data. Then, we statistically compared observed and surrogate data across subjects by means of a dependent-samples t-test. We used the Monte Carlo method with 1000 repetition. This step was done independently for each time-frequency-grid point sample. Next, we combined data points with a p-values < 0.05, which were adjacent in time, frequency, and space to a cluster. We pre-defined a neighbour structure for the data, which contains the positions of the channel and its relative neighbours and restricted the neighbours to be maximum 0.6 cm away. Minimum cluster size was set to two.

To obtain the surrogate cluster distribution, we calculated p-values for each time-frequency-grid point and repetition, by testing every surrogate value against the other surrogate values of that time-frequency-grid point. We defined clusters with the same parameters as described for the observed data. This process was repeated 1000 times, always selecting the largest surrogate cluster found. This resulted surrogate cluster distribution was used to test the observed data against it (see table S1).

In an additional post hoc analysis, we investigated if power had a systematic influence on our reported phase effects (see Results). We median split the threshold SOA trials into low and high-power trials and calculated the POS values as described above. We averaged the POS values for each participant over the channel-time-frequency points where we found phase effects. We applied a t-test to test for systematic differences between phase values between high and low power trials.

Phase dependent behavioural performance

The POS analysis provides information on whether the phase of neuronal oscillations differs between correct and incorrect trials. For a more detailed understanding of the relationship between prestimulus phase and performance accuracy, we calculated the participants' fractal accuracy for different phase bins. To this end, we first determined in each participant the time-frequency sample with the highest POS value within the grid points belonging to the significant cluster in the POS analysis (Baumgarten et al., 2015). For this time-frequency sample, we computed the momentary phase for each threshold SOA trial (see above for the parameters). Next, we binned the phase values from -π to +π in steps of $\frac{1}{3}\pi$. For each of these six phase bins, we calculated the individual performance averaged across all trials. We normalized individual performance by subtracting the mean of all bins from each bin. Next, we aligned the bins so that the bin with the highest performance was aligned to bin zero. Finally, we averaged data per bin across participants. To test for statistical significance, we performed a one-way repeated ANOVA, while bin 0 was excluded from the statistics, and post hoc Tukey-Kramer tests for pairwise comparisons between phase bins. The average trial count per bin was for bin one 27.7 (± 7.7 SD), bin two 28.2 (± 8.2 SD), bin three 26.0 (± 7.4 SD), bin four 29.6 (± 8.6 SD), bin five 27.2 (± 7.4 SD) and bin six 28.5 (± 6.7 SD).

Phase dependent ERF

We investigated whether prestimulus phase affects visual stimulus processing. To this end, we used an early visual components of the event related field (ERF) – the N170/N1 component - as a measure of stimulus processing (e.g., Mazaheri and Picton, 2005; Han et al., 2015). The individual latency of the component was based on a data driven approach. We took the first component in our data, which had a negative deflection at around 170 ms., hence we called it N170 component. First, we determined 100 grid points showing the highest ERF values. To this end, we calculated for each grid point t-values for the ERF by applying a dependent sample t-test between post-stimulus ERF (0 s to 0.3 s) and prestimulus ERF (averaged across -0.8 s to -0.5 s) and selected 100 grid points showing the highest absolute t value averaged across 170 ms ± 25 ms.. The N170 component was therefore based on an average of times points, this was done to account for varying time point between subjects. Next, from these 100 selected channels, we computed for each participant the momentary phase for the threshold SOA trials. We binned the phase as described above and re-calculated the ERF t values, this time only for the trials within each bin. We averaged the ERF t value across all 100 grid points for each participant and aligned the highest value to bin zero. Finally, we averaged the t-values per bin over participants and performed a one-way repeated measure ANOVA, excluding bin with phase 0, and post hoc Tukey-Kramer tests for pairwise comparisons between phase bins (see table S1). The average trial count for the six bin was for bin one 26.5 (± 8.0 SD), bin two 27.5 (± 6.3 SD), bin three 29.1 (± 8.6 SD), bin four 30.2 (± 8.3 SD), bin five 26.3 (± 7.5 SD) and bin six 27.5 (± 7.0 SD). We additionally visualised the averaged ERF time course for three different phase bins. The ERF data was first phase binned with the same binning method as described above, and then aligned to phase bin zero. The difference is that the data was not averaged over the N170 component but the complete time course is used. Additionally we tested if the phase binning of the behavioural analysis (see above), leads to similar results. This would indicate that the phase, relevant for the behavioural effect also directly effects the ERF amplitude. Therefore, we sorted the ERF trials based on the phase values of the behavioural data. Then the ERF values were binned and aligned to phase bin 0.

Correlation of peak frequency with threshold SOA

Previous studies reported a correlation between participants' perceptual temporal resolution and the peak frequency of neuronal oscillations (e.g., Samaha et al., 2015). Based on these findings, we tested if the individual peak frequency correlates with the SOA derived from the staircase and the theoretical fitted SOA. For the theoretical fitted SOA, we fitted a sigmoid function onto the individual behavioural data using the Palamedes toolbox for MATLAB (Prins and Kingdom, 2018). From the fitted function, we computed the SOA for which the participant reached 50% correct responses. This SOA, we call the fitted threshold SOA. We used this second approach to account for potential noise in the initial threshold SOA estimation. We estimated the peak frequency for each participant not based on power values but on the highest POS value. To this end, we selected within the significant cluster in the POS analysis the frequency of the highest POS value per participant (using the Matlab function findpeaks.m). Finally, we correlated (Pearson's correlation) the estimated individual peak frequencies with the individual threshold SOA estimated during the staircase and with the fitted SOA (fitted SOA). Additionally, we fitted a general linear model onto the data for visualization. We are aware that this is not a conventional method to investigate the influence of peak frequency on the temporal integration window (Baumgarten et al., 2017b; Cecere et al., 2015; Samaha and Postle, 2015; Tarasi and Romei, 2023). Therefore, we ran a complementary analysis to detect power peaks, correlated them with the staircase, and fitted threshold SOA. The prestimulus power spectrum was calculated using a single Hanning window with a frequency resolution of 2 Hz, between 2 and 30 Hz. With the FOOOF toolbox (Version 1.1.0) (Donoghue et al., 2020), we corrected for the 1/f component. We determined for each virtual channel the frequency with the highest power using findpeaks.m. We calculated the average peak frequency for the cluster channels, for each subject, and correlated those with the staircase and fitted SOA.

Code Accessibility

The analysis was run on Linux using Matlab (R2019b), using a 40 core computer with 120 GB Ram, operating system is debian 10 (buster). Due to their large size, the data files will be made available upon request. Analysis scripts are made unrestricted available, and can be found following this link: https://osf.io/ah3gf/?view_only=0d058e3560cf4eeeafdee337f6ab8c22

Results

Participants performed a visual temporal discrimination task in which they were presented with two grids partially filled with annuli separated by SOAs of varying duration. If both grids were integrated, only one position was not filled with an annulus. Participants' task was to report by button press whether they detected the empty position, i.e., whether they were able to temporally integrate both stimuli.

Behavioural results

In a staircase procedure prior to the experiment, we determined the SOA, at which participants were able to detect the empty position in 50% of the trials (60.0 ± 7.7 ms; mean ± SEM). The average threshold SOA was 60 ms (± 38.45 ms, range 16 – 144 ms). In the main experiment, we determined recognition rates as a function of different SOAs (short, threshold SOA, long, intermediate plus and minus SOAs, see Methods). For short SOA, recognition rates were at 0.80 ± 0.03 (mean ± SEM); for intermediate minus at 0.55 ± 0.04 (mean ± SEM), for threshold SOA at 0.45 ± 0.03 (mean ± SEM), intermediate plus at 0.42 ± 0.03 (mean ± SEM) and long SOA at 0.31± 0.04 (mean ± SEM) (Fig. 11). A one-way ANOVA revealed a significant main effect of SOAs ($F = 20.9$, $p < 0.001$; Fig. 11). Post hoc Tukey-Kramer tests showed that the short SOA differed significantly from all other SOAs (all pairwise comparisons $p < 0.001$). The intermediate minus SOA differed significantly from the intermediate plus SOA ($p = 0.013$) and the long SOA ($p = 0.004$). Post hoc tests showed no significant differences between intermediate minus SOA and threshold SOA ($p = 0.212$), threshold SOA and intermediate plus SOA ($p = 0.769$), threshold SOA and long SOA ($p = 0.564$), and intermediate plus SOA and long SOA ($p = 0.999$)

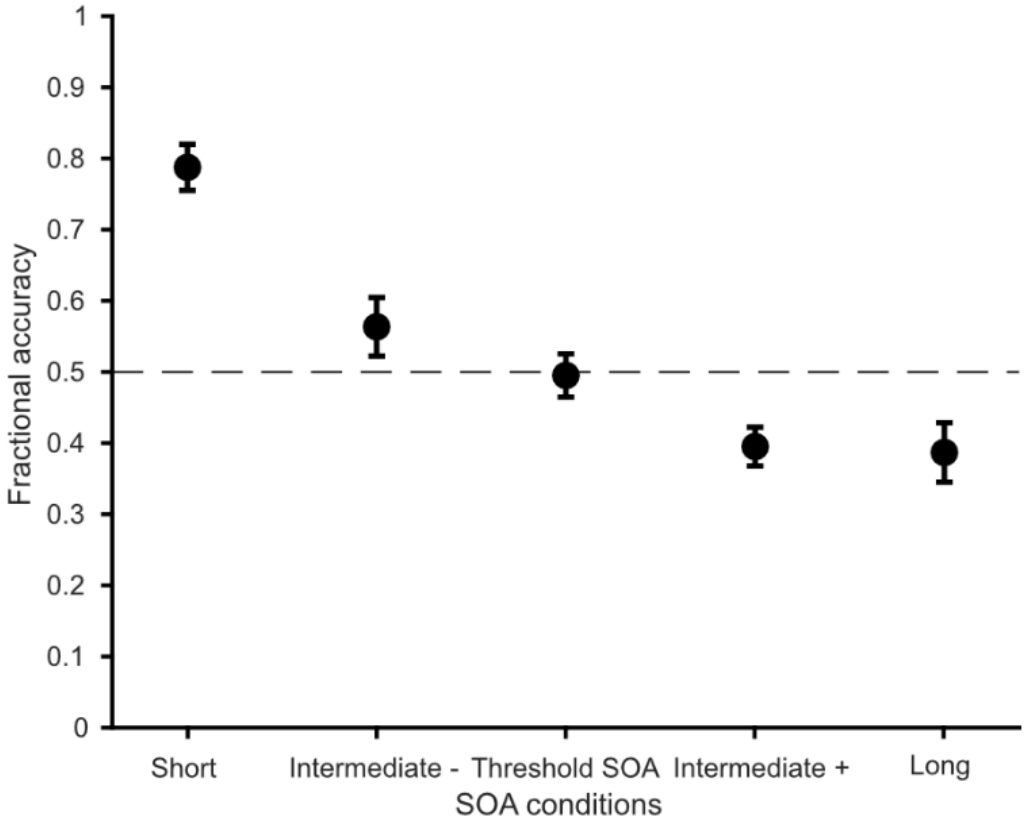

Figure 11 Behavioural performance. Fractional accuracy is plotted against the different SOA conditions. The dashed line marks the 50 % mark indicating the performance level we expected to see for the threshold SOA. Data are presented as mean ± SEM. A one-way ANOVA reveals a significant effect of SOA conditions ($p < 0.001$).

Phase contrasts

To investigate whether perception is influenced by the phase of neuronal oscillations, we split all trials with a threshold SOA according to participants' perception (i.e., correct, and incorrect trials). Next, we analysed putative phase differences between correct and incorrect trials by computing the phase opposition sum (POS, VanRullen, 2016) on source level for each time-frequency-grid sample and subsequently performing a cluster-based permutation test. The average trial count for correct trials was mean = 87.4 (± 34.343 STD) and for incorrect trials mean = 81.2 (± 25.146). The results revealed a significant cluster ($p = 0.048$, summed t-values: 2722.4, t-value range: [2.07 6.57]) between -0.8 s to -0.5 s and between 6 Hz to 20 Hz, showing the most pronounced effect between 8 Hz and 16 Hz (Fig. 12B). The significant cluster was located at the *parietal lobe* (Fig. 12A left), and more prominent in the left hemisphere (Fig. 12A, right).

We tested for systematic POS differences between high and low power trials, by recalculating the POS values for high and low power trials. We averaged the POS values per subject for the channel-time-frequency points we reported above. We found no power difference between POS values (t = -0.61, p = 0.577).

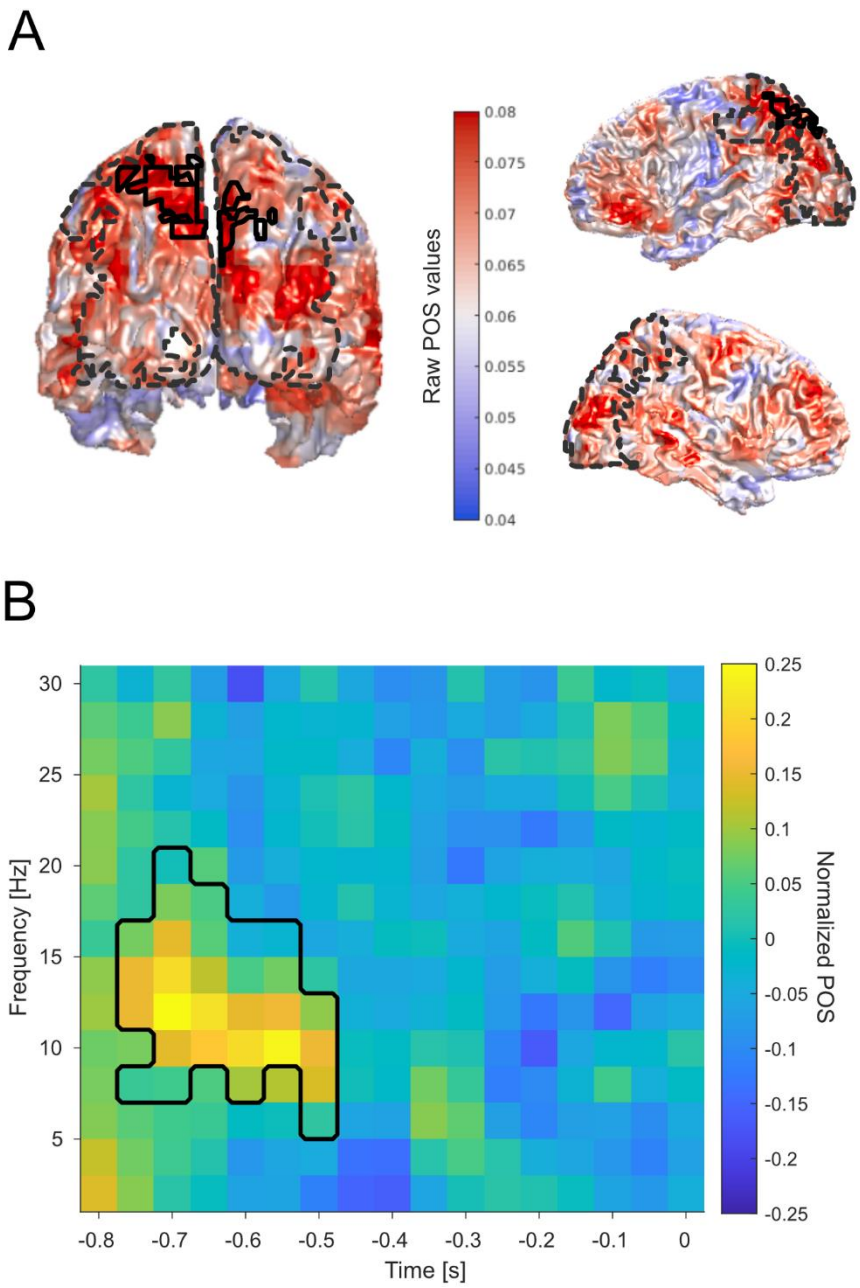

Figure 12 Phase opposition sum (POS) effects. A) POS values projected on a template MNI brain viewed from posterior (left) and right and left view (right). The black outline indicates the significant region/virtual channels (p = 0.048, summed t-values: 2722.4, t-value range: [2.07 6.57]. The dashed line indicates the region of interest for statistical comparison. B) Averaged normalized phase opposition values over all significant virtual channels of the cluster (see A). The black outline indicates the significant time-frequency range.

Phase and behavioural performance

We investigated how behaviour was modulated by the momentary phase. To this end, we computed for each participant the phase for all trials at the time-frequency sample showing the highest POS value. Next, we binned single trials according to their momentary phase in six bins and averaged for each bin participants' responses (Fig. 13). A one-way ANOVA excluding the phase bin containing the aligned highest responses (bin 0) revealed a significant effect of phase bin on accuracy (F = 3.9, p = 0.005). A post hoc Turkey-Kramer test showed a significant difference between bin π and bin $\frac{1}{3}\pi$ (p = 0.035) and between bin $-\frac{1}{3}\pi$ and bin $\frac{1}{3}\pi$ (p = 0.003), and a trend towards significance difference between bin $-\frac{2}{3}\pi$ and $\frac{1}{3}\pi$ (p = 0.053). We additionally restricted the analysis to the alpha band (8-12 Hz), following the same pipeline but with a different frequency range of interest. The results showed no significant influence of phase on behaviour, when restricted to the alpha phase (F = 0.58, p = 0.681).

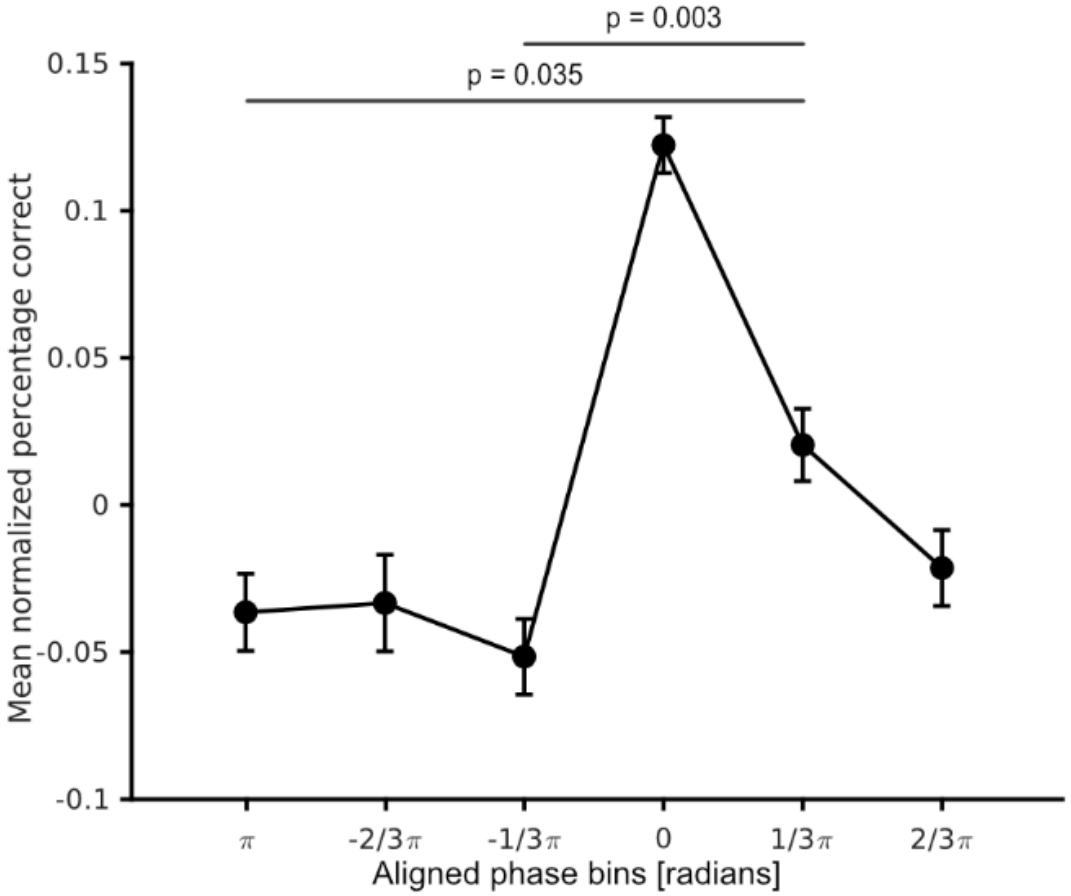

Figure 13 Phase dependence of behaviour. Normalized fractional accuracy plotted against the binned prestimulus phase. Data are shown as mean ± SEM. An ANOVA revealed a significant effect of phase bins (F = 3.87, p = 0.005). Black lines indicate significant differences between phase bins in post-hoc pairwise comparisons.

Phase and ERF

We binned trials according to their momentary phase in equally spaced phase bins. Next, we computed per participant the ERF t values for all trials in each bin and averaged the ERF t values across participants. The ERF t values were obtained by contrasting the baseline period (-0.8 s to -0.5 s) with the post stimulus time period of interests (0 s to 0.3 s). A one-way ANOVA showed a significant effect of phase bins (F = 3.4, p = 0.011; Fig. 14 right). A post hoc Turkey-Kramer test showed a significant difference between bin $-\frac{1}{3}\pi$ and bin $\frac{2}{3}\pi$ (p = 0.016) and a trend towards a significance between bin $-\frac{1}{3}\pi$ and bin $\frac{1}{3}\pi$ (p = 0.064). Additionally, we tested if these effects were also found, when restricted to the alpha band. We performed the same analysis, but this time we calculated the momentary phase between 8 – 12 Hz and not between 2 – 30 Hz, as we did before. Our additional analysis showed that there was no difference between phase bins when restricted to the alpha band (F = 1.98, p = 0.102). When visually inspecting the averaged ERF curves for two different phase bin, we saw a clear amplitude difference (Fig. 14 left). Single subject data is shown as extended data (Appendix Supplementary Fig. S1). At last, our analysis of binning the ERF t values based on the phase values used for the behavioural data, revealed the same qualitative pattern, but no significant effect of phase bin on ERF t values (F =1.53, p =0.199).

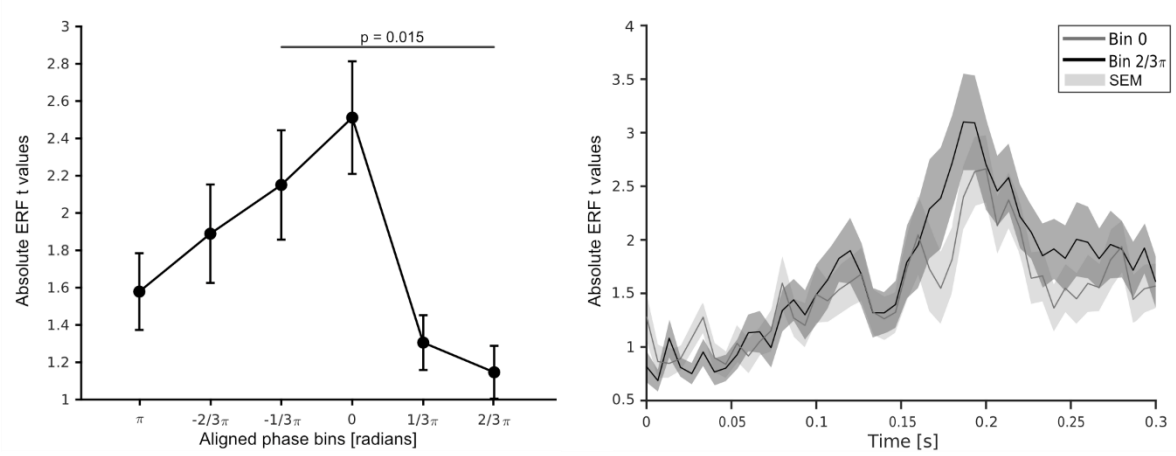

Figure 14 Phase dependence of ERF amplitude. A) ERF t values plotted against the binned pre stimulus phase. Data are shown as mean ± SEM. An ANOVA revealed a significant effect of phase bins (F = 3.4, p = .011). Black lines indicate significant differences between phase bins in post-hoc pairwise comparisons. B) ERF amplitude as absolute ERF t values are shown for two phase bins. Bin 0 in light grey and bin $\frac{2}{3}\pi$ in black. The shaded are is the standard error of mean. No statistics were applied, only for visualization. See figure 5-1 for individual ERF data.

Correlation of peak frequency and threshold SOA

We investigated whether the individual peak frequency correlates with individual threshold SOA. Therefore, we correlated peak frequency with the estimated SOA prior to the experiment (staircase) (Fig. 15A) and the fitted (Fig. 15B) threshold SOA (see Methods for details). For three participants the fitted threshold SOA could not be determined reliably ($R^2 < 0.33$). These participants had to be excluded from the respective correlation analysis. We did not find any significant correlation between individual peak frequencies and staircase threshold SOAs ($r = 0.25$, $p = 0.26$) nor between peak frequencies and fitted threshold SOA ($r = 0.18$, $p = 0.43$). As for our supplementary analysis, where we correlated power peak frequency with the threshold and fitted threshold SOA, we found no significant correlation between either staircase ($r = -0.1$, $p = 0.64$) nor the fitted threshold SOA ($r = -0.24$, $p = 0.24$). Lastly, we restricted the frequency range of interest of our initial analysis to the alpha band 8-12 Hz, this restriction did not change the results. For the staircase threshold SOA ($r = 0.25$, $p = 0.26$) nor for the fitted threshold SOA ($r = 0.18$, $p = 0.43$) was a significant correlation found for the peak frequency.

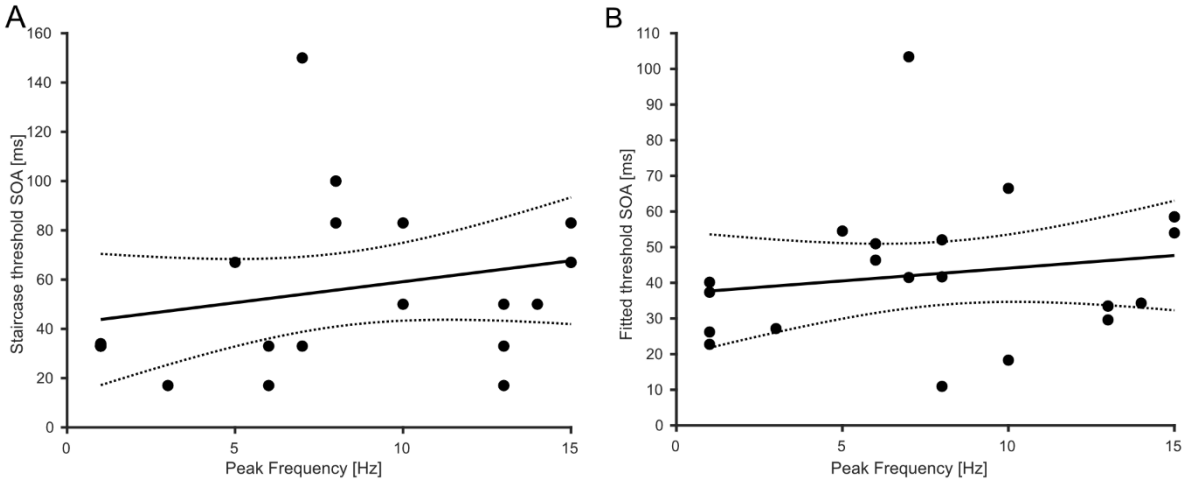

Figure 15 Correlation between peak frequency and threshold SOAs. A) Threshold SOA determined prior to the experiment plotted against the peak frequency (see Methods for details). Pearson correlation revealed no significant correlation ($r = 0.25$, $p = 0.26$). B) Same as A) but this time correlation between estimated fitted threshold SOA and peak frequency (see Methods for details). Pearson correlation revealed no significant correlation ($r = 0.18$, $p = 0.423$). The black line represents the linear regression, the dotted lines the 95% confidence intervals for the mean.

Discussion

There is an ongoing debate whether prestimulus phase of neuronal oscillations influences perception (e.g., Keitel et al., 2022; Harris, 2023). Most evidence favouring a crucial role of phase stems from visual detection tasks, here, we investigated how prestimulus phase modulates visual temporal integration. We found phase differences when comparing correct with incorrect trials. These phase effects were in the frequency range between 6-20 Hz, and - 0.8 to -0.5 s prior to stimulus presentation, mainly in parieto-occipital areas. Additionally, accuracy decreased when deviating from the preferred prestimulus phase. Finally, prestimulus phase modulates poststimulus visual processing as the N170 amplitude attenuated when deviating from the individually preferred phase. However, we found no evidence that the individual frequency of the prestimulus phase correlates with the temporal integration threshold.

Previous studies investigating visual detection tasks reported phase effects in the alpha-band (Busch et al., 2009; Kraut and Albrecht, 2022; Landau and Fries, 2012b; Mathewson et al., 2009; Zazio et al., 2022), in our study the effects are largest in the range 8-16 Hz, but also exceeding to the low beta-band (20 Hz). It remains an open question whether these broadband effects stem from averaging inter-individual differences or represent a genuine broadband effect. Visual inspection of the results on single subject level, could not give a clear answer in either direction. Thus, our analysis seems not suited to investigate this broadband effect further. However, the higher frequencies in our study might depend on task demands. It has been reported that alpha peak frequency shifts to higher frequency in cognitively more demanding tasks (Haegens et al., 2014). Similarly, studies have shown that occipital alpha peak frequencies differ between visual integration or segregation task (Han et al., 2023; Sharp et al., 2022; Wutz et al., 2018). Relevant frequency shifted with task difficulty also in a visual search task (Merholz et al., 2022). In line with these findings, the higher frequencies here reported might be explained by higher task difficulty of a temporal discrimination task compared to detection tasks. On the other hand, Wutz et al. found differences of peak frequencies between the integration and segregation task. They found slightly lower peak frequency for the integration task compared to the segregation task. (Wutz et al., 2018). It could be that the task demand was slightly higher for the segregation task compared to the integration task (see slightly lower maximum recognition rates).

While most studies report phase effects over the occipital lobe (Alexander et al., 2020; Fakche et al., 2022; Wutz et al., 2018; Zazio et al., 2022), we found phase effects in the parietal lobe. One possible explanation could be that higher order visual areas are involved in solving this task. A classical hypothesis states that the “where” pathway – which processes information about the spatial location of objects - includes the parietal lobe (Mishkin et al., 1983). A potential reason for effects in the parietal lobe might be that these areas are engaged in our spatial integration and detection task.

The reported performance effects (decreasing when deviating from preferred phase) are smaller compared to other studies (~7% difference between highest and lowest bin compared to ~13%, Busch et al., 2009; Dugue et al., 2011; Baumgarten et al., 2015; Fakche et al., 2022). Task difficulty could be a leading cause for the difference, while the effect pattern is comparable. In addition, we found that prestimulus phase modulates the amplitude of the poststimulus N170 component. In line with our finding, prestimulus phase has been reported to modulate global field potential (Busch and VanRullen, 2010; Dou et al., 2022; note that Dou et al. found these effects only for high power trials), TMS-evoked ERPs (Fakche et al., 2022; Romei et al., 2012), and visual awareness negativity (Krasich et al., 2022). In sum, these studies suggest across a variety of different tasks that prestimulus phase can modulate poststimulus components. However, we found that the prestimulus phases in different, but overlapping areas modulate behaviour and the amplitude of the N170 component. For the behavioural data, we looked for prestimulus phase values of the highest POS values and for the ERF data, we searched for the phase values of the 100 channels showing the highest ERF amplitude. It could be that modulation of behaviour and ERF amplitude happen at separated areas.

While our results are comparable to detection task results, the underlying mechanism is not well understood. Earlier studies proposed the idea that stimulus presentation triggers a phase shifted towards a preferred phase, inducing a phase reset (Makeig et al., 2002). When prestimulus phase is at the preferred phase, stimulus processing is optimal, leading to increased evoked responses and improved performance. Whereas, when phase has to shift toward the preferred phase, processing is less optimal, leading to decreased evoked responses and behaviour. This could be investigated by comparing phase angle values before and after phase reset. Such analyses, however, might be practically less straightforward due to potential temporal smearing effects by the methods for phase analysis (Brüers and VanRullen, 2017).

Neuronal phase might also indicate the current excitability of the underlying neuronal population (Bishop, 1932; Fakche et al., 2022; Lakatos et al., 2007). In theory, cortex excitability changes rhythmically with phase, while excitability is highest at a preferred phase (Jensen and Mazaheri, 2010; Mazaheri and Jensen, 2006; Schaworonkow et al., 2019). Neuronal processing would be facilitated at such a preferred phase and putatively lead to higher ERPs. Stimulus processing would be more effective and putatively lead to better behavioural performance. Cortical excitability has also been repeatedly linked to the power of alpha oscillations (e.g. Romei et al., 2008; Lange et al., 2013; Dou et al., 2022). Here, low alpha power is beneficial for perception, while high alpha power suppresses excitability. Notably, phase effects on behaviour and neuronal processing have often been reported for high but not for low alpha power trials (Alexander et al., 2020; Dou et al., 2022; Fakche et al., 2022; Mathewson et al., 2009; Ozdemir et al., 2022). The reason could be, when power is low, cortical excitability is high and phase effects are less notably or irrelevant. In contrast, when power is high, excitability is low and phase matters more strongly as excitability differs more strongly between different phases.

Between studies, there is a high variability regarding the latency of the reported phase effects. Some report effects close to stimulus onset (~ 100-200 ms before stimulus onset; e.g.,(Alexander et al., 2020; Fakche et al., 2022; Zazio et al., 2022) other studies – including the present study - report phase effects several 100 ms before stimulus onset (Baumgarten et al., 2015; Hanslmayr et al., 2013; Kraut and Albrecht, 2022). We can only speculate about the causes of these discrepancies. One reason might be that the timing of effects depends on the task (see above discussion on the frequency band). Temporal smearing effects of peri- or poststimulus effects into the prestimulus period (Brüers and VanRullen, 2017) might also overshadow putative phase effects close to stimulus presentation. Another explanation could be that slow frequencies orchestrate faster frequency. Evidence stems from reported power-phase coupling between higher and lower frequencies (Axmacher et al., 2010; Canolty et al., 2006; Palva, 2005; Voytek, 2010). Similarly, studies have reported phase-phase-coupling of neuronal oscillations in different frequency bands (Belluscio et al., 2012; Scheffer-Teixeira and Tort, 2016). Underlying (ultra-)slow oscillation orchestrating alpha activity on a network level would lead to a rhythmic occurrence of phase effects, with a visible component several ms before stimulus presentation.

Respiration could be such a slow oscillation, by increasing the overall oxygen level, which would lead to higher excitability. Respiration has an effect on behavioural measures (Johannknecht and Kayser, 2022) and modulates alpha power at rest and during detection tasks (Kluger et al., 2021a; Kluger et al., 2021b). In addition, the slow cardiac cycle influences neuronal activity and behavioural performance rhythmically (Al et al., 2020; Kim et al., 2019). Such slow fluctuations have also been reported for perception (e.g., Monto et al., 2008; Palva and Palva, 2012). By investigating longer prestimulus periods of several seconds, future studies might shed more light on such rhythmic patterns and how they affect phase and other components of neuronal oscillations.

Finally, we investigated if a specific frequency band is relevant for unimodal visual temporal integration. Recent studies found evidence for a correlation between individual alpha peak frequencies and behavioural performance in visual or multimodal studies (Bastiaansen et al., 2020; Keil and Senkowski, 2017; Migliorati et al., 2020; Minami and Amano, 2017; Samaha and Postle, 2015; Venskus et al., 2021; Venskus and Hughes, 2021). A common interpretation of such correlations is that the cycle of a neuronal oscillation might reflect temporal integration windows, while the frequency shapes the window size. Following a slightly different approach, by taking the frequency with the highest individual phase effect (Baumgarten et al., 2015), we found no evidence for an influence of frequencies on perception or temporal integration.

While several studies reported an effect of phase on perception in different tasks, interpretations about the functional role of phase differ. In short, two hypotheses exist: the hypothesis of rhythmic perception states that the intensity or probability of perception changes rhythmically with phase (VanRullen, 2016a; VanRullen and Koch, 2003). The hypothesis of discrete perception states that the phase relative to stimuli determines whether the stimuli fall within the same or different perceptual cycles leading to different perceptions (Baumgarten et al., 2015; VanRullen and Koch, 2003). Our results show that phase correlates with behaviour and post-stimulus ERFs, while we found no support for perceptual cycles. Therefore, we suggest that unimodal visual temporal integration is a rhythmic process, in a wider frequency range as expected, and potentially even modulated by even slower underlying oscillations.

A limitation of this study is that the estimation of individual phase effects is typically less stable as determining peak frequencies. Such noisy estimation might influence the results.

In addition, we observed high subject variability in the behavioural data and phase opposition effects (absolute value, timing, frequency). Our analysis captures the overlapping effects on group level. Other study designs would be more suited to capture individual differences.

In addition, it should be noted that several studies report null findings with respect to phase effects on perception or neuronal activity (Melcón et al., 2023; Michail et al., 2022; Ruzzoli et al., 2019; Zazio et al., 2022). Here, we can only speculate about the discrepancies. In our study, phase effects were very local in space (see also Palva, 2005; Baumgarten et al., 2015). In addition, typically phase effects are smaller than power effects. Therefore, phase effects might be too small to be detected or overshadowed by other effects, especially when analysed on sensor level, as spatial leakage of other effects might be stronger than the actual phase effect. It also seems that phase effects are only visible in tasks near the perceptual threshold, but not for easier tasks. It remains to be studied whether phase plays a continuous role in our perception or is only relevant near the perceptual threshold. Finally, potential phase effects might be overlooked due to methodological problems in the analyses (Harris, 2023).

In conclusion, we found an effect of phase of alpha oscillations in a visual temporal discrimination task and on neuronal processing. These results suggest that perception is a rhythmic process and/or that the phase modulates stimulus processing. While these results are of correlative nature, future studies might investigate causal relationships between phase and perception/neuronal processing. To test a putative causal relationship, phase resets could be triggered externally and the consequences on behaviour can be tested.

Study Two: Subliminal visual stimulation produces broadband behavioural oscillations in a visual integration task

Contributions

Michelle Johannknecht: Conceptualized research, performed research, analysed the data and wrote the manuscript

Prof. Dr. Alfons Schnitzler: Wrote the manuscript

PD Dr. Joachim Lange: Wrote the manuscript

Published 20th January 2025 in Scientific Reports; DOI: https://doi.org/10.1038/s41598-025-85385-5

Abstract

We perceive our surrounding as a continuous stream of information. Yet, it is under debate, whether our brain processes the incoming information also continuously or rather in a discontinuous way. In recent years, the idea of rhythmic perception has regained popularity, assuming that parieto-occipital alpha oscillations are the neural mechanism defining the rhythmicity of visual perception. Consequently, behavioural response should also fluctuate in the rhythm of alpha oscillations (i.e., at ~10 Hz). To test this hypothesis, we employed a visual integration task. Crucially we investigated if a subliminal stimulus preceding the target stimulus modulates behaviour. Our results show that behaviour fluctuates as a function of delay between subliminal and target stimuli. These fluctuations were found in the range of theta, alpha and beta oscillations. Our results further support the idea, that alpha oscillations are a functional rhythm for visual perception, leading to rhythmic fluctuations of perception and behaviour. In addition, other frequencies seem to play a role for temporal perception.

Introduction

In our everyday life, we receive a continuous influx of information from our surrounding. A long-standing question is whether this information is also processed continuously by our senses. In recent years, the idea of non-continuous perception has gained new popularity. The idea of non-continuous perception states that our visual system works in a rhythmic or discrete manner (VanRullen and Koch, 2003). Rhythmic perception assumes that stimulus perception is good or less good in certain phases of an

underlying rhythm (VanRullen, 2016a). Discrete perception assumes the existence of perceptual integration windows.

Incoming information will be perceptually integrated or segregated depending on whether the information fall within one common or within separate perceptual windows (Baumgarten et al., 2015). Both theories – rhythmic and discrete perception - have in common that in their view perception is not a continuous process but rather fluctuates rhythmically over time. It has long been proposed that neuronal oscillations might form the neural basis for rhythmic perception, a theory that has regained popularity in the last years (Busch and VanRullen, 2010; Dou et al., 2022; Harter, 1967; Keitel et al., 2022; Valera et al., 1981). Especially, due to their dominant presence in the visual system, alpha oscillations (i.e., ~8-12 Hz) are assumed to be the underlying neuronal rhythm for creating rhythmic visual perception (VanRullen, 2016a). Therefore, visual perception should fluctuate in the frequency of the underlying alpha oscillation.

Indeed, there is evidence that behavioural responses fluctuate rhythmically. For example, when a visual test stimulus follows a salient, but irrelevant visual stimulus, detection of a test stimulus fluctuates rhythmically (~ 4 Hz) as a function of the distance between test and irrelevant stimulus[(Landau and Fries, 2012a; Song et al., 2014)]. Similar rhythmic behaviour has been shown for simple visual tasks (Fiebelkorn and Kastner, 2019; Landau and Fries, 2012b; Re et al., 2019; Song et al., 2014) and more complex visual stimuli in context of image familiarity (Liu and Melcher, 2023). Also, for multisensory tasks, studies found rhythmic behaviour. When participants listened to a task irrelevant auditory stimuli and solved then a visual task, behavioural performance fluctuate at ~4-8 Hz (Plöchl et al., 2022). While these studies reported rhythmic fluctuations of behaviour, the reported rhythms were often in the range of 4-8 Hz, i.e. in the theta-range. According to the theory of perceptual cycles, however, perceptual processes should fluctuate at the intrinsic frequency relevant for perception in the respective sensory modality, i.e. in the alpha-range for the visual system (~8-12 Hz) (VanRullen, 2016a). Indeed, most studies assigned the rhythmicity of responses in the theta-range to attentional processes rather than perceptual processes.

While these salient, supra-threshold stimuli can help to understand how attentional resources fluctuate over time and influence behaviour, behavioural fluctuations due to perceptual processes might be overshadowed and not visible. To overcome this problem, subliminal stimuli might be helpful. Subliminal stimuli are physically present

but below a perceptual threshold such that observers do not consciously perceive these stimuli. Subliminal stimuli thus unlikely trigger (covert) attentional processes.
Although not consciously perceived, subliminal stimuli produce neural activity in early sensory areas, but not in higher order areas (Blankenburg et al., 2003; Dehaene et al., 2006). Subliminal stimuli might thus influence perception of subsequent stimuli. Previous studies in the tactile domain used subliminal tactile stimuli and found behavioural fluctuations in the beta-range (13-17 Hz) (Baumgarten et al., 2017a). For the tactile (Blankenburg et al., 2003; Forschack et al., 2020; Iliopoulos et al., 2020; Nierhaus et al., 2015) as well as visual domain (Bareither et al., 2014; Schwartz and Rem, 1975; Silverstein et al., 2015; Sperdin et al., 2015; Wu et al., 2009) neural signatures of subliminal stimuli have been investigated. While it is not fully clear if the observed neural signatures are best characterized by short lived burst of activity[(Bareither et al., 2014)] or whether they are actually long lasting (Silverstein et al., 2015), there is evidence that these stimuli can effect behaviour in various domains (Bareither et al., 2014; Blankenburg et al., 2003; Ferrè et al., 2016; Iliopoulos et al., 2020; Mudrik and Deouell, 2022; Taskin et al., 2008). It has to be noted that studies differ in experimental design, the type of subliminal stimuli they are using and the conceptualization of what is a consciously perceived stimulus (Mudrik and Deouell, 2022).
In the present study, we want to investigate putative rhythmic perceptual processes in the visual system. While most studies focused on detection tasks, we employed a visual temporal integration task (Wutz et al., 2016). To disentangle perceptual from attentional processes, we use subliminal stimuli preceding the test stimuli. Similar to previous studies (Chen et al., 2017; Fiebelkorn et al., 2011; Landau and Fries, 2012a; Re et al., 2019; Song et al., 2014), we expect that behavioural responses fluctuate rhythmically as a function of temporal distance between subliminal and test stimulus. Due to the use of subliminal (instead of supraliminal stimuli) (Chen et al., 2017; Fiebelkorn et al., 2011; Landau and Fries, 2012a; Re et al., 2019; Song et al., 2014), we expect to find fluctuations at the frequency relevant for visual temporal integration, i.e. the alpha rhythm.

Material and Methods

Subjects

We recruited 20 participants. We excluded one data set, because of some hardware delays causing the sampling delays to be imprecise. Therefore, 19 data sets were analysed (9 females, mean age 25.4 ± 5.2 years SD). One participant was left-handed. All participants had normal or corrected to normal vision and declared to have no neurological disorder. The study was conducted according to the declaration of Helsinki and approved by the ethics committee of the University clinic Düsseldorf. Participants were compensated with 13€/hour.

Paradigm

In a nutshell, we used a visual temporal integration task, which could be solved only if two stimuli separated by a temporal delay were successfully integrated (Johannknecht et al., 2024). Crucially, the task stimuli were preceded by a subliminal stimulus with varying delays between subliminal and task stimuli.

In more detail (Figure 16 A), during a prestimulus period the dark grey screen was shown for a random duration between 600 and 800 ms. Next, a fixation cross was shown for a duration of 1000 ms. Within this period, additionally the subliminal stimulus was shown for 16 ms at a random time point between -600 ms and -312 ms (in steps of 16 ms). After the fixed fixation period of 1000 ms, the two task stimuli were shown. The two task stimuli consisted each of seven full and one-half annuli placed on random positions of a 4 x 4 grid. If both images were superimposed, all grid positions were filled except one empty location (see below for a detailed description). Each image was shown for 16 ms and the images were separated by an SOA. We used different SOA condition similar to previous studies (Baumgarten et al., 2017a). The different SOA condition consisted of a short SOA of 0 ms (i.e., both images shown in direct succession), the threshold SOA obtained from the staircase (see below for a description), two intermediate SOAs where (i.e. threshold SOA ± 16 ms; called intermediate plus/minus) and a long SOA condition (threshold SOA ± 48 ms) (Figure 16 B). In each block, we presented for each subliminal-target-delay 10 trials of the threshold SOA and 1 each of the intermediate plus and minus condition and of the long and short SOA in pseudo-random order. After both target stimuli were presented, the fixation cross was shown for a random duration between 600 - 1200 ms.

Afterwards the participants had to report the position of the column and the row of the empty location by pressing buttons with the right hand. First, they reported the column by pressing one of four buttons. Next, they reported the row, again by pressing one of four buttons. After the response or if no response was given within 4000 ms, the next trial started.

We additionally included catch trials for the subliminal stimulus, which were randomly interspersed between the other trials. In these catch trials, only the subliminal stimulus was presented, and participants were asked if they had seen the stimulus. They had to response “yes” or “no”, by pressing one of two buttons on the response button box. The buttons were randomly assigned to the answer choice. We used real and fake catch trials, during real catch trials the actual subliminal stimulus was presented and during fake catch trials the fixation cross on the dark grey background was continuously presented. There was a 10 % chance that a trial could be a catch trial. Fake and real catch trials appeared with 50 % chance, each.

To increase the number of trials, we split the experiment in two separate sessions, each on a separate day. For each session, we repeated the two staircases. Each session included 20 trials of the threshold SOA per sampling delay (380 trials per session) and two trials of the other SOA condition per sampling condition (38 trials combined for the other SOA condition per session). One session lasted between 45 and 60 minutes of recording. The participant did a short training session of 2 to 5 minutes before starting the experiment.

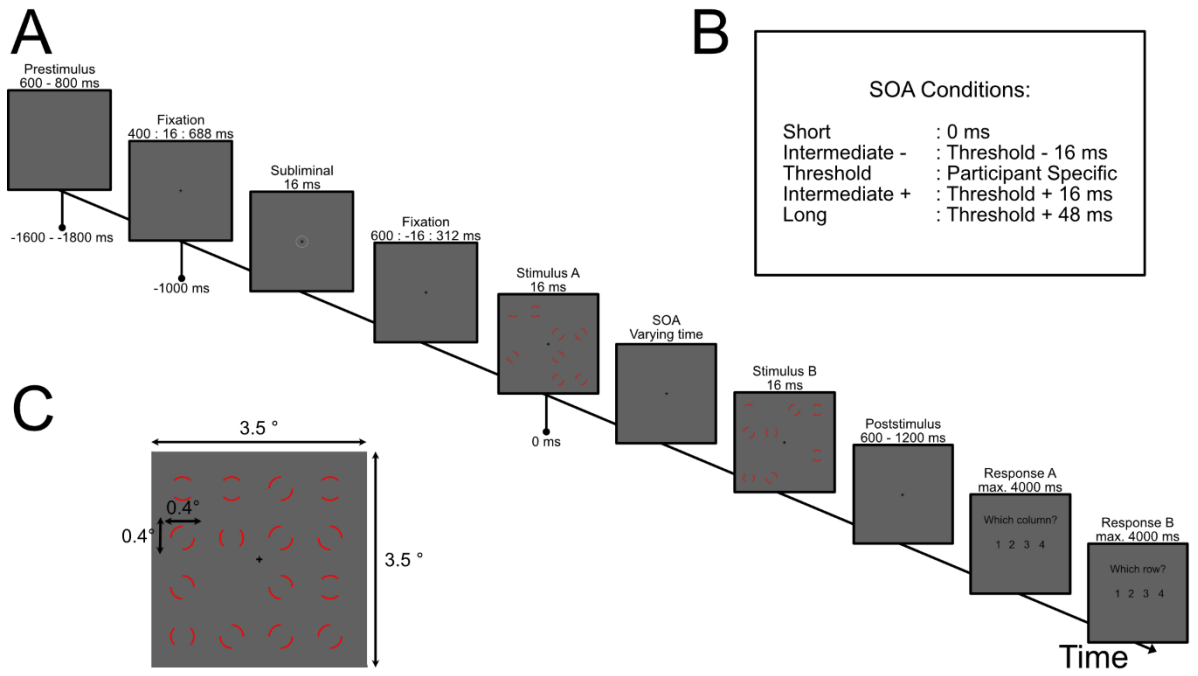

Figure 16: Paradigm study two. (A) The experiment started with a prestimulus period where only a dark grey screen was shown (for 600-800 ms). Afterwards, a fixation cross was presented for 1000 ms. Within these 1000 ms, additionally a subliminal stimulus was shown for 16 ms (one frame) at random positions between 312 and 600 ms before the test stimulus. The subliminal stimulus consisted of a ring around the fixation cross (visual angle 0.8°). Its grey value was adjusted to the perception level of the participant. Next, the two test stimuli were shown for 16 ms, each with a varying stimulus offset asynchrony (SOA) (see B for SOA condition). A poststimulus period followed, where a fixation cross was shown for 600 ms up to 1200 ms. Then the first and second response prompt followed (each could be displayed for up to 4000 ms). (B) The different SOA condition used in this experiment. The threshold SOA was individually defined to achieve 50% accuracy. (C). An example of a fully integrated test stimulus.

Stimuli

The task stimulus consisted of two separate, complementary images. Each image had seven full and one-half red [RGB 1 0 0] annuli placed on random positions of a 4 X 4 grid on a dark grey background [RGB .38 .38 .38]. In the centre of each image was a black [RGB 0 0 0] fixation cross (Fig. 16 C). When both images are superimposed, all positions of the 4 X 4 grid are filled except one empty location. The size of the grid was 8 cm by 8 cm (visual angle of 3.5° by 3.5°). Each annulus was 1 cm by 1 cm, and evenly spaced on the grid (Figure 16 C). Twenty test stimuli (i.e., 40 single images in total) were generated prior to the experiment.

The subliminal stimulus was a ring around the fixation cross. The ring had a diameter of 1.8 cm (visual angle of 0.8°). The colour value of the circle ranged between 0.38 (no contrast to the background, 0 % Weber contrast) to 0.57 (high contrast, 40 % Weber contrast). The colour value was adapted individually in a staircase method (see below), so that the stimulus was just not consciously perceived.

The stimuli were presented via a projector (Panasonic, PT-DW700E; 60 Hz refresh rate) and projected onto a translucent screen using a mirror system. The screen was 140 cm in front of the participant. Stimulus presentation was controlled by the software Presentation (Neurobehavioral System, Albany NY, USA).

Staircase

Prior to the experiment, we ran two separate staircase procedures: In one staircase procedure, we defined the contrast threshold of the subliminal stimulus. In the other staircase procedure, we defined the threshold stimulus onset asynchrony (SOA) for the task stimuli.

In the staircase for the contrast threshold, we presented the participant on each trial only the subliminal stimulus. The starting RGB value was 0.47, so the contrast difference is around 21.2 % (Weber contrast). The subliminal stimulus was presented for 16 ms and participants had to report via button press if they have seen the stimulus ("yes" or "no"). After each "yes" the grey value was decreased by .01 (contrast decreased by 2.6 %). When the participant reported ten times in a row "no", the grey value of the increased by .01 (contrast increased by 2.6 %). If the participant reported 20 times in a row "no", the staircase terminated, and the momentary grey value was taken as the value for the subliminal stimulus in the subsequent main paradigm. In between trials, stimuli with random grey values were presented to the participant. These randomly chosen stimuli were not evaluated during the staircase. Participants had to respond either with their index finger or with middle finger. We assigned the response choice (yes/no) randomly to these two buttons for each trial.

During the staircase for the SOA of the task stimuli, we presented the participant only the task stimuli. Participants' task was to find the empty location in the 4 X 4 grid of annuli. This task could be solved only by superimposing both images. Participants reported the position in two steps: First, they had to press one of four buttons on a button box to report the column. In the second step, they had to press the same buttons to report the row. The stimuli were presented for 16 ms, each, separated by a SOA. The starting SOA was always set to 26 ms. When the participant reported twice in a row the correct position, the SOA was increased by 16 ms. When the participant answered twice in the row incorrectly, the SOA decreased by 16 ms. If the SOAs of the last 20 trials was stable (i.e. variance < 0.5), the staircase terminated, and the momentary SOA was taken as the threshold SOA in the subsequent main paradigm.

In between trials, random SOAs (between 0 ms and 144 ms, in steps of 16 ms) we presented. These randomly chosen SOAs were not evaluated during the staircase.

Behavioural analysis and statistics

Data was analysed in Matlab (Version R2023b) using the FieldTrip Toolbox (Version 20210825) (Oostenveld et al., 2011) or in Python (Version 3.10.12) using Google Collaboratory.

First, we analysed each participants' responses as a function of SOA between the two target stimuli and then averaged performance across participants. To this end, we pooled the response per SOA across all subliminal-target-delays. This analysis was done for each session separately. To test for a systematic difference in accuracy across SOA or across sessions, we ran an ANOVA with post-hoc pairwise comparisons (Tukey Kramer test).

Additionally, we evaluated the performance for the catch trials, by calculating for each session the average "yes" response per participant and then averaged across participants. To test for significant differences, we ran an ANOVA.

Second, for each participant and subliminal-target-delay, we calculated the accuracy for the threshold SOA trials. The data was then linearly detrended and demeaned. The analysis was done separately for each subject and session. Then the data was zero padded to 1 second and we computed a fast Fourier transform on the data. Because we sampled the subliminal-target-delay every 16 ms, our frequency resolution was 60 Hz, so the Nyquist frequency was 30 Hz, therefore the FFT was performed between 1 and 29 Hz. We used for each time window a single taper resulting in a spectral smoothing of 3 Hz. Afterwards the power spectrum of the behavioural data was averaged across sessions and then across participant.

To test whether the power spectrum showed significant peaks (i.e., behavioural data fluctuated rhythmically), we compared the spectra to surrogate data. First, we constructed surrogate data by shuffling the accuracy values (raw values) randomly in time and repeated this 1000 times. For each repetition we detrended and demeaned the data and then calculated an FFT with the same settings as for the observed data. We calculated the median of the surrogate repetition per subject and then averaged over session per subject (Baumgarten et al., 2017a; Fiebelkorn et al., 2011; Landau and Fries, 2012a).

Because this method of time shuffling received some critic (Brookshire, 2022), we used two additional methods to generate surrogate data. First, we created random accuracy data per sampling delay. Second, we used an autoregression method for generating surrogate data.

For the random accuracy surrogate dataset, we simulated data separately for each participant and session. For each sampling delay, we modelled response values randomly as “correct” or “incorrect”. The number of repetitions at each sampling delay was identical to the number of trials in the observed data. Since observed behavioural data showed that performance was not perfect at 50 % accuracy for the threshold SOA, we added an offset to the random accuracy values. This offset was based on the average performance of the respective participant in that session for the threshold SOA. Afterwards, we averaged the resulting random accuracy values across repetitions per sampling delay and repeated this step 1000 times. For each repetition, we calculated an FFT with the same setting as described above and then calculated the median of the surrogate receptions of the power values and averaged over session, for each participant separately. This procedure was inspired by a shuffling procedure by VanRullen (VanRullen, 2016b), while we did not shuffle between groups but between two possible outcomes.

The AR model was constructed in Python based on Brookshire (Brookshire, 2022). We used the “statsmodel” module and constructed an ARIMA process with an autoregression parameter of 1:

$$X_t = c + \Phi X_{t-1} + \varepsilon_t \quad (3)$$

Where X_t is the modelled response, c is a constant, Φ the autoregression constant, X_{t-1} the data at time point t minus one and finally, ε_t is noise (Brookshire, 2022; Liu and Melcher, 2023). The input for the model was the detrended accuracy data. The noise is based on the standard deviation of the residuals estimated by the model. Based on the estimated parameters from the model for each subject and session an ARMA (Auto Regressive Moving Average) process was modelled, from this we generated 1000 surrogate data sets with the same length as the original data set. This data was then saved and imported to Matlab, where we calculated for each repetition the FFT, after detrending and demeaning the data. The median of the surrogate repletion was calculated and the averaged over session for each participant.

For all three approaches, we tested the observed data against the surrogate data by means of a cluster- based permutation test (Maris and Oostenveld, 2007). The procedure was identical for all three sets of surrogate data. First, we used a t-test to statistically compare for each frequency the power values of the observed data and the surrogate data. Then, we applied a threshold (t = 1.734, alpha = 0.05) to the t-values and t-values of neighbouring frequencies exceeding this threshold were clustered. The t-values within each cluster were summed and this value served as the cluster statistic of the observed data. Next, we shuffled randomly power values between observed and surrogate data sets. This was done 10000 time and for each repetition cluster statistics were computed as described above. For each repetition, the largest cluster was selected. Afterwards we compared the observed cluster with the surrogate cluster distribution and calculated the respective p values.

Results

Participants performed a visual temporal integration task in which task stimuli were presented with varying SOAs and an empty location on a 4x4 grid had to be detected. The task could only be solved, if the two stimuli were perceptually integrated. Crucially, the two task stimuli were preceded by a subliminal stimulus with varying delay before the task stimuli. To increase number of trials, participants performed the task in two sessions on two separate days.

Group level performance

First, we tested statistically if session and/or SOA between the task stimuli influence the behavioural performance of the participants. We found a statistically significant main effect of SOA condition ($F = 13.27$, $p < 0.01$) but no effect of session ($F = 1.48$, $p = 0.226$) and no interaction effect ($F = 0.64$, $p = 0.637$) (Figure 17 A). Post hoc multi-comparison test (Turkey Kramer test) revealed a significant difference between the short SOA and threshold SOA ($p < 0.01$), between the short SOA and the intermediate plus SOA ($p < 0.01$), between the short SOA and the long SOA ($p < 0.01$), between the intermediate minus SOA and the long SOA ($p < 0.01$) and finally between the threshold SOA and the long SOA ($p < 0.01$).

Responses to subliminal stimuli

Next, we analysed if participant did not perceive the subliminal stimulus. We statistically compared participants' "yes" (i.e. seen) reports in the real and fake catch trials. We found no significant effect of catch trial type (fake vs. real) ($F = 0.81$, $p = 0.372$) or session ($F = 0.04$, $p = 0.84$) and no significant interaction effect ($F = 0.15$, $p = 0.7$) (Figure 17 B).

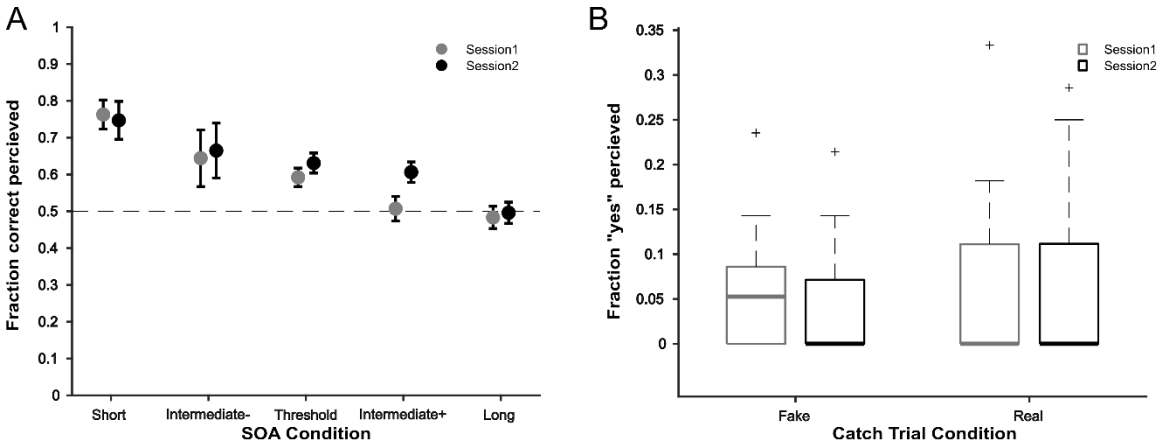

Figure 17 Behavioural data. (A) Group level results of the accuracy as a function of SOA. Data are shown individually for each session. The dashed line indicates 50% accuracy. The black lines indicate the standard error of the mean. The results of an ANOVA showed no main effect of SOA condition on the accuracy ($F = 13.27$, $p < 0.01$) but an effect of session ($F = 1.48$, $p = 0.226$), and no interaction effect ($F = 0.64$, $p = 0.637$). (B) Results for the catch trials for each condition. Data are shown individually for each session. Fake catch trials were catch trials without a subliminal stimulus presented and real catch trials with a subliminal stimulus presented. The thick line within the boxes indicate the median. An ANOVA shows no effect of catch trial condition ($F = 0.81$, $p = 0.372$), session ($F = 0.04$, $p = 0.84$) and no interaction effect ($F = 0.15$, $p = 0.7$).

Rhythmic behaviour

Finally, we analysed whether participants' performance fluctuates rhythmically as a function of delay between subliminal stimulus and target stimuli(Baumgarten et al., 2017a). The results of the cluster-based permutation test revealed for each surrogate data set significant positive clusters. Positive t-values indicate stronger rhythmicity in this frequency compared to the surrogate distribution (Figure 18). For the time shuffled data set, we found a significant cluster between 1-3 Hz (cluster statistic = 8.3, $p < 0.01$), between 10 -13 Hz (cluster statistic = 8.4, $p < 0.01$) and between 19-21 Hz (cluster statistic = 6.2, $p < 0.01$). For the random accuracy surrogate data, again we found three positive clusters between 1-3 Hz (cluster statistic = 9.3, $p < 0.01$), between 10-13 Hz (cluster statistic = 8.8, $p < 0.01$) and 19-21 Hz (cluster statistic = 6.4, $p < 0.01$). For the AR shuffling again, we found three positive clusters 1-5 Hz (cluster statistic = 21.82, $p < 0.01$), between 9-15 Hz (cluster statistic = 22.24, $p < 0.01$) and between 17-24 Hz (cluster statistic = 20.92, $p < 0.01$).

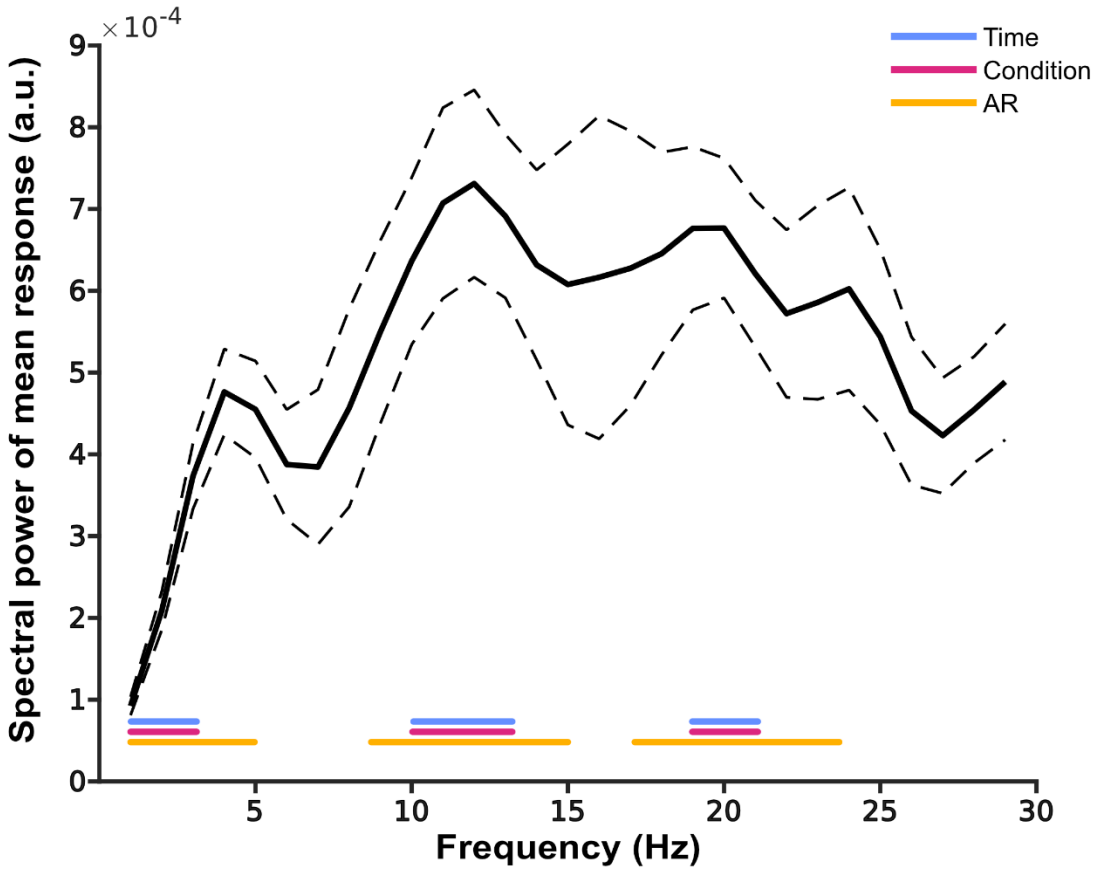

Figure 18 Spectral power of the responses (thick line: mean across participants, dashed line: standard error of the mean). Coloured lines at the bottom indicate frequencies, which are significantly different from the random surrogate data (all $p < 0.01$). The different colours indicate the different methods used to generate surrogate data (see Methods for details).

Discussion

In this study, we analysed the effect of subliminal stimulation on the behavioural response in a visual integration task. We applied three different methods to produce surrogate data, ensuring that the analysis pipeline itself did not artificially bias our results. Independent of analysis pipeline, we found behavioural fluctuation, in a delta/theta frequency range (1–3 Hz), in the alpha range (9-15 Hz) and in the beta range (17-24 Hz). Our initial hypothesis was that the frequency of behavioural oscillations should match the frequency of relevant oscillations in the respective modality. That is, we expected to find behavioural oscillations mainly in the alpha range. While our results confirm this hypothesis, we also find behavioural oscillations in the theta- and beta-range.

We found behavioural oscillation in the range of the assumed relevant neural oscillation, similar to the study of Baumgarten et al. (Baumgarten et al., 2017a). In their study, Baumgarten et al. (Baumgarten et al., 2017a) investigated tactile discrimination ability. They presented, two suprathreshold tactile stimuli separated by a stimulus offset asynchrony and participant had to discriminate between two or one perceived stimuli. Prior to the tactile discrimination task, a subliminal tactile stimulus was presented at different time delays between subliminal and suprathreshold stimuli. Baumgarten et al. reported behavioural oscillation between 13 – 24 Hz, i.e. in the beta range, supporting their hypothesis that for the somatosensory domain beta oscillations are the functional frequency sampling tactile perception. In line with this hypothesis, we found behavioural oscillations in the range of the functional frequency in the visual modality, i.e. in the alpha range.

Studies using visual tasks reported behavioural oscillations, in the alpha and at higher frequencies (Liu and Melcher, 2023; Song et al., 2014). Song et al. (Song et al., 2014) used a visual discrimination task preceded by an above threshold cue. They reported behavioural oscillations at a frequency of 2 - 5 Hz, confirming previous studies (Landau and Fries, 2012a). Interestingly, behavioural performance also showed fluctuations in the alpha-/beta range (8-20 Hz). Song et al. (Song et al., 2014) concluded that the slow oscillation samples spatial locations and the alpha oscillation is involved in the attentional sampling process. Liu and Melcher (Liu and Melcher, 2023), investigated in a memory task if face familiarity modulates behavioural oscillation in a gender discrimination task, showing either familiar or unfamiliar faces.

They found slow oscillations (2.7 Hz) for unfamiliar faces and high oscillations (12.9 Hz) for familiar faces. They concluded that task demand could influence perceptual sampling. Wutz et al. used the same task as we did in the present study. They found that alpha oscillations were modulated by task demands, i.e., whether participants' task was to integrate or segregate the stimuli (Wutz et al., 2018).

In addition to the alpha rhythm, we found behavioural fluctuations at slower frequencies (~1-3 Hz). Slower oscillations in behavioural performance have been associated with attention mechanism (Fiebelkorn et al., 2011; Landau and Fries, 2012b; Re et al., 2019), with supra threshold stimuli attracting the attention of the observer. In our study, we used subliminal stimuli to modulate perception. The rationale to use subliminal stimuli was to avoid such covert attentional processes that putatively overshadow potential perceptual processes at alpha rhythms. A crucial question is whether the subliminal stimulus was indeed not consciously perceived. By presenting only subliminal stimuli interspersed between the main paradigm, we aimed to control whether the subliminal stimuli were perceived. Our data show that we can be confident that the subliminal stimulus was indeed below perceptual threshold.

While we carefully controlled that the subliminal stimuli were not consciously perceived and do not attract covert attention, it seems that our task still involved some kind of attention. Studies have shown that suprathreshold stimuli that were not consciously perceived could still modulate attention (Bareither et al., 2014; Mudrik and Deouell, 2022). While not being consciously perceived, also subliminal stimuli might involve some kind of (unconscious and overt) attentional processes. These overt attentional processes might be reflected in the slow oscillations of behaviour in our task. Alternatively, It might be that attention fluctuates naturally over time (Mooneyham and Schooler, 2013) and we caught these natural fluctuations with our task. Wutz et al. used the same task as we did in the present study, but participants had to perform either an integration task as in our study or a segregation task. Wutz et al. found an oscillation the theta-band (3-7 Hz) in the prestimulus period. Whether stimuli were integrated or segregated depended on a phase shift in this oscillation (Wutz et al., 2018).

Finally, we also found behavioural oscillations in the range of beta oscillations. In a previous study, we used the same task but without presenting a subliminal stimulus prior to the task stimulus. In this study, we measured neural activity with MEG in addition to the behavioural performance.

We found that participants' behaviour (i.e. correct vs. incorrect identification of the empty location) correlated with the phase of neuronal oscillations in the range of alpha oscillations, but the effect also extended to the beta oscillations (8-20 Hz (see Johannknecht et al., 2024)). Other studies found that task difficulty could modulated the range of frequency functionally relevant for modulating behaviour. More difficult tasks or higher task demands could shift the frequency relevant for the task to higher frequencies up to beta frequencies (Chen et al., 2017; Liu and Melcher, 2023; Merholz et al., 2022). An alternative explanation could be inter-individual differences between participants. When comparing the individual behavioural spectra, we can see that some participants show only one peak (in the alpha or beta range), others multiple peaks. It could be that individually experienced task difficulty is reflected in different frequencies of behavioural fluctuations.

In sum, all these different factors could explain the differences in the individual spectra resulting in three different peaks on group level. While the behavioural fluctuations in the alpha-range confirm our initial hypothesis, other frequency ranges might also be functionally relevant for temporal visual perception.

At this moment, we can only speculate about the mechanism how the subliminal stimulus modulates behavioural responses. Previous studies assumed that supra-threshold stimuli can reset the phase of the ongoing neuronal oscillation and thus lead to fluctuations of behaviour (Fiebelkorn et al., 2011; Tosato et al., 2022). In addition, it has been reported that subliminal stimuli can induce evoked response (Bareither et al., 2014; Forschack et al., 2020; Nierhaus et al., 2015; Silverstein et al., 2015) and phase resets of neuronal oscillations (Palva, 2005), which might lead to behavioural fluctuations (Baumgarten et al., 2017a). In the present study, we additionally recorded neural activity with MEG. An obvious next step in a future study is to analyse these data with respect to putative phase resets of neuronal oscillations induced by the subliminal stimulus and its putative relation to the behavioural fluctuations.

Additionally, future studies might directly compare the influence of subliminal and suprathreshold stimuli on behaviour and neural activity. Such comparisons might shed new light on the processes underlying covert/overt attentional sampling and perceptual sampling.

Conclusion

In the present study, we showed that a subliminal stimulus could induce fluctuations of participants' performance in a visual temporal discrimination task. We found that behavioural performance fluctuated in the alpha rhythm, as well as at slow theta rhythms and comparably high beta rhythms. These results are in line with the hypothesis that our visual system operates non-continuously. The data, however, do not allow us to distinguish whether the underlying process is a rhythmic facilitation or a discrete process. In further studies, we will analyse electrophysiological data to investigate if prestimulus alpha phase modulates temporal visual perception.

Data Availability

Behavioural data will made public, as well as the code the data was analysed with. The scripts for pre-processing are available as well so that interested readers can understand how the data was handled before analysis. The data and code can be found under following link:
https://osf.io/j8sxp/?view_only=79f9f15691ac4858886217a24018495a

General Discussion

Summary

The first study examined alpha oscillations' influence on successfully integrating two temporally separated images. The hypothesis posited that the phase of alpha oscillations in the occipital lobe before stimulus presentation modulates our ability to integrate the images. In a visual temporal integration task, subjects reported the location of a missing object within a pattern, requiring successful integration of both images. Concurrently, brain signals were recorded using MEG. The study sought to determine whether correct and incorrect trials were associated with opposite phase angle values by comparing the momentary phase prior to stimulus presentation. Furthermore, the study investigated the relationship between behaviour and the momentary phase and amplitude of early visual components. Additionally, it examined the correlation between the temporal window of integration and the individual peak frequency of the subjects. The results affirmed that the phase of alpha oscillations significantly influences behavioural performance and the amplitude of early visual components. These phase effects also extended into the beta range.

It was noted that performance and amplitude decreased when deviating from the individual preferred phase. No correlation was found between the subjects' integration window and peak frequency.

The second study sought to investigate the impact of subliminal stimuli on subjects' behavioural performance in a temporal visual integration task. The hypothesis was that the subliminal stimulus would lead to fluctuations in behavioural performance in the alpha range. Before the temporal integration task, a subliminal visual stimulus was presented. The study analysed the behavioural performance as a function of the time delay between subliminal stimulus and task stimulus. The results showed that behavioural performance fluctuated in the delta/theta, alpha, and beta range, with these fluctuations being significantly distinct from random data.

Conclusion

Based on the first study's results, I can conclude that our visual temporal perception is rhythmic. The phase of prestimulus oscillation affects the successful integration of temporally separated images. It seems that post-stimulus processes modulate the success of integration because the prestimulus phase modulates event-related amplitude, an indicator of the strength of stimulus processing.

In study two, I also found evidence for a rhythmic process. Behavioural processes fluctuated rhythmically. This rhythmicity was elicited by presenting a subliminal stimulus before showing the test stimulus. This could indicate that the subliminal stimulus successfully modulated the underlying oscillation, leading to behavioural fluctuations. Modulating the underlying oscillation by resetting the phase would modulate only the oscillation phase, not the oscillation frequency. In other words, the value of the phase changes abruptly once; however, no additional cycles per time unit are added to change the frequency of the oscillation. This further supports the notion that this process is rhythmic and not discrete.

Previous studies explored the influence of prestimulus oscillation on the detectability of single visual stimuli. These studies reported phase effects in the alpha band (Busch et al., 2009; Kraut and Albrecht, 2022; Landau and Fries, 2012a; Mathewson et al., 2009; Zazio et al., 2022), similar to the results in my first study. Effects were located in the occipital lobe (Alexander et al., 2020; Fakche et al., 2022; Wutz et al., 2018; Zazio et al., 2022), comparable to my results.

However, the reported timing of the effects in the prestimulus period differed (Alexander et al., 2020; Baumgarten et al., 2015; Fakche et al., 2022; Hanslmayr et al., 2013; Kraut and Albrecht, 2022; Zazio et al., 2022) to my reported latencies. When focussing on the behavioural data, studies reported mainly slow oscillatory frequencies (Landau and Fries, 2012; Re et al., 2019; Song et al., 2014) that seem to modulate attention. In my second study, behaviour fluctuated also in higher frequencies. However, data from the tactile domain suggest that subliminal stimuli can modulate also higher frequencies (Baumgarten et al., 2017a).

With the accumulated evidence, I can conclude that temporal visual processing is rhythmic. The phase of the underlying oscillation modulates event-related potential along the visual hierarchy. Using subliminal stimuli, I shifted the phase of the underlying oscillation, leading to behavioural fluctuations. However, some points remain open for discussion.

Frequency range

I initially anticipated that the alpha frequency would be the exclusive modulator of visual processing. However, in study one, I observed phase effects within the beta range (13-30 Hz). I also noted behavioural oscillations in the beta and delta/theta ranges (1-5 Hz) in study two. Previous studies have mainly reported effects within the alpha range (Kraut and Albrecht, 2022; Mathewson et al., 2009; Zazio et al., 2022), but some have also reported rhythmic effects in faster (Busch et al., 2009; Kraut and Albrecht, 2022; Landau and Fries, 2012a) or slower (Brüers and VanRullen, 2017) frequency ranges.

The beta frequency indicates faster local processes, suggesting that local modules along the visual hierarchy are engaged. These local processes also seem to be modulated by the prestimulus phase. Slower oscillations in behavioural tasks are often associated with attentional mechanisms. It is possible that the subliminal stimulus could unconsciously modulate the observer's attentional resources. Given that several other frequencies are essential for the task's success and several processes influence our temporal perception, attention may also play a part in this task. Participants reported high attention demands and overall difficulty with the task.

Latency of effect

In my first study, I observed effects occurring as early as 800 ms before the onset of the first task stimulus. However, I had expected to see phase effects closer to the onset of the task stimulus. In contrast, other studies have shown variations in latencies from close to stimulus presentation (Alexander et al., 2020; Fakche et al., 2022; Zazio et al., 2022) to effects several hundred milliseconds prior to stimulus presentation (Baumgarten et al., 2015; Hanslmayr et al., 2013; Kraut and Albrecht, 2022). One possible explanation for the lack of effects near the onset of the stimulus is that phase effects may be overshadowed by event-related potentials induced by the stimulus presentation. Another hypothesis is that even slower oscillations influence the phase effects themselves. As hypothesised in the second study, behavioural performance may also be modulated by slower attentional fluctuations, suggesting that slower oscillations drive internal processes in our visual system. I speculated in the first study that these slow oscillations originate from bodily functions, such as fluctuations in blood oxygenation levels (Palva and Palva, 2012). Therefore, the surprising early occurrence of phase differences in driving behaviour could be explained by the fact that other slow oscillations drive the overall excitability of our visual system on a much slower time scale. However, further research is needed to investigate these phase effects by expanding the pre-stimulus period in future studies to make any strong claims.

Location

I anticipated observing phase differences in early visual areas in the occipital lobe, as indicated by previous studies (Alexander et al., 2020; Fakche et al., 2022; Wutz et al., 2018; Zazio et al., 2022). However, in study one, phase effects extended into the parietal lobe. This suggests that locations along the dorsal pathway may also process information relevant to solving this task. The dorsal pathway is responsible for processing spatial information about perceived objects. It is plausible that the spatial information necessary to solve the task involving the missing object is also processed in this pathway. The task may activate multiple areas in the visual hierarchy, as shown by the phase effects in the occipital and parietal lobes.

Limitations

A limitation of these studies is the high variability of subjects. Single-subject data showed individual patterns in both studies. Study one included frequency, space and timing of the observed phase effects. For study two, these subject-specific effects were observed in the frequency peak in the behavioural data. For both studies, threshold SOA values varied between subjects but also between sessions (in case of study two). Both studies were not designed to capture individual effects, and the trial number per subject is too low to investigate individual effects. A within-subject design would be necessary to investigate these individual observed effects. However, our analysis is designed to capture group-level effects. Even with subject variability, overlapping effects result in significant group-level effects, as reported in my two studies. Another limitation specific to study one is the estimation of phase effects itself. Phase estimations suffer from poor signal-to-noise ratios, as the phase estimation I used is directly impacted by trial number. I made sure to thoroughly clean the data and have sufficient trial numbers in this study. However, the inherent sensitivity of this measure should be noted.

Last, specifically for study two, the claimed unobserved subliminal stimulus is challenging to prove based on subjective reports of the participants. Future studies would benefit from directly comparing the neuronal response of a subliminal stimulus and a suprathreshold stimulus. Additionally, behavioural data alone makes the proposed phase reset hard to prove. The rhythmic behaviour indicates this proposed phase reset; however, future studies must prove this with recoded neuronal data to estimate phase values before and after the subliminal stimulus and compare these two groups.

Outlook

In studies one and two, I discovered evidence indicating that temporal visual integration is a rhythmic process. In study two, evidence suggests that subliminal stimuli can influence behavioural responses. A logical next step would be to investigate whether the subliminal stimuli used lead to the hypothesised phase reset (as discussed in the introduction) and if the phase effects reported in study one can be replicated or modified using the paradigm of study two. We can use the MEG to capture processed information in our visual system with high temporal and spatial resolution. Conducting this additional study could help establish a causal relationship between the phase of pre-stimulus oscillation and our perception, deepening our understanding of how our perception integrates information over time and further elucidating our visual experiences of the world.

References

Al, E., Iliopoulos, F., Forschack, N., Nierhaus, T., Grund, M., Motyka, P., Gaebler, M., Nikulin, V.V., Villringer, A., 2020. Heart–brain interactions shape somatosensory perception and evoked potentials. Proc. Natl. Acad. Sci. U.S.A. 117, 10575–10584. https://doi.org/10.1073/pnas.1915629117

Alexander, K.E., Estepp, J.R., Elbasiouny, S.M., 2020. Effects of Neuronic Shutter Observed in the EEG Alpha Rhythm. eNeuro 7, ENEURO.0171-20.2020. https://doi.org/10.1523/ENEURO.0171-20.2020

Axmacher, N., Henseler, M.M., Jensen, O., Weinreich, I., Elger, C.E., Fell, J., 2010. Cross-frequency coupling supports multi-item working memory in the human hippocampus. Proc. Natl. Acad. Sci. U.S.A. 107, 3228–3233. https://doi.org/10.1073/pnas.0911531107

Baillet, S., Mosher, J.C., Leahy, R.M., 2001. Electromagnetic brain mapping. IEEE Signal Process. Mag. 18, 14–30. https://doi.org/10.1109/79.962275

Bareither, I., Chaumon, M., Bernasconi, F., Villringer, A., Busch, N.A., 2014. Invisible visual stimuli elicit increases in alpha-band power. Journal of Neurophysiology 112, 1082–1090. https://doi.org/10.1152/jn.00550.2013

Bastiaansen, M., Berberyan, H., Stekelenburg, J.J., Schoffelen, J.M., Vroomen, J., 2020. Are alpha oscillations instrumental in multisensory synchrony perception? Brain Research 1734, 146744. https://doi.org/10.1016/j.brainres.2020.146744

Baumgarten, T.J., Königs, S., Schnitzler, A., Lange, J., 2017a. Subliminal stimuli modulate somatosensory perception rhythmically and provide evidence for discrete perception. Sci Rep 7, 43937. https://doi.org/10.1038/srep43937

Baumgarten, T.J., Schnitzler, A., Lange, J., 2017b. Beyond the Peak – Tactile Temporal Discrimination Does Not Correlate with Individual Peak Frequencies in Somatosensory Cortex. Front. Psychol. 8. https://doi.org/10.3389/fpsyg.2017.00421

Baumgarten, T.J., Schnitzler, A., Lange, J., 2016. Prestimulus Alpha Power Influences Tactile Temporal Perceptual Discrimination and Confidence in Decisions. Cereb. Cortex 26, 891–903. https://doi.org/10.1093/cercor/bhu247

Baumgarten, T.J., Schnitzler, A., Lange, J., 2015. Beta oscillations define discrete perceptual cycles in the somatosensory domain. Proceedings of the National Academy of Sciences 112, 12187–12192. https://doi.org/10.1073/pnas.1501438112

Belluscio, M.A., Mizuseki, K., Schmidt, R., Kempter, R., Buzsáki, G., 2012. Cross-Frequency Phase–Phase Coupling between Theta and Gamma Oscillations in the Hippocampus. J. Neurosci. 32, 423–435. https://doi.org/10.1523/JNEUROSCI.4122-11.2012

Benwell, C.S.Y., Coldea, A., Harvey, M., Thut, G., 2022. Low pre-stimulus EEG alpha power amplifies visual awareness but not visual sensitivity. Eur J of Neuroscience 55, 3125–3140. https://doi.org/10.1111/ejn.15166

Bishop, Geo.H., 1932. CYCLIC CHANGES IN EXCITABILITY OF THE OPTIC PATHWAY OF THE RABBIT. American Journal of Physiology-Legacy Content 103, 213–224. https://doi.org/10.1152/ajplegacy.1932.103.1.213

Blankenburg, F., Taskin, B., Ruben, J., Moosmann, M., Ritter, P., Curio, G., Villringer, A., 2003. Imperceptible Stimuli and Sensory Processing Impediment. Science 299, 1864–1864. https://doi.org/10.1126/science.1080806

Brookshire, G., 2022. Putative rhythms in attentional switching can be explained by aperiodic temporal structure. Nat Hum Behav 6, 1280–1291. https://doi.org/10.1038/s41562-022-01364-0

Brüers, S., VanRullen, R., 2017. At What Latency Does the Phase of Brain Oscillations Influence Perception? eNeuro 4, ENEURO.0078-17.2017. https://doi.org/10.1523/ENEURO.0078-17.2017

Busch, N.A., Dubois, J., VanRullen, R., 2009. The Phase of Ongoing EEG Oscillations Predicts Visual Perception. Journal of Neuroscience 29, 7869–7876. https://doi.org/10.1523/JNEUROSCI.0113-09.2009

Busch, N.A., VanRullen, R., 2010. Spontaneous EEG oscillations reveal periodic sampling of visual attention. Proc. Natl. Acad. Sci. U.S.A. 107, 16048–16053. https://doi.org/10.1073/pnas.1004801107

Buzsáki, G., 2006. Rhythms of the brain. Oxford University Press, Oxford ; New York.

Buzsáki, G., Anastassiou, C.A., Koch, C., 2012. The origin of extracellular fields and currents — EEG, ECoG, LFP and spikes. Nat Rev Neurosci 13, 407–420. https://doi.org/10.1038/nrn3241

Buzsáki, G., Wang, X.-J., 2012. Mechanisms of Gamma Oscillations. Annu. Rev. Neurosci. 35, 203–225. https://doi.org/10.1146/annurev-neuro-062111-150444

Canolty, R.T., Edwards, E., Dalal, S.S., Soltani, M., Nagarajan, S.S., Kirsch, H.E., Berger, M.S., Barbaro, N.M., Knight, R.T., 2006. High Gamma Power Is Phase-Locked to Theta Oscillations in Human Neocortex. Science 313, 1626–1628. https://doi.org/10.1126/science.1128115
Cecere, R., Rees, G., Romei, V., 2015. Individual Differences in Alpha Frequency Drive Crossmodal Illusory Perception. Current Biology 25, 231–235. https://doi.org/10.1016/j.cub.2014.11.034
Chen, A., Wang, A., Wang, T., Tang, X., Zhang, M., 2017. Behavioral Oscillations in Visual Attention Modulated by Task Difficulty. Front. Psychol. 8, 1630. https://doi.org/10.3389/fpsyg.2017.01630
Clarke, J., 1994. SQUIDs. Scientific American 271, 46–53.
Dehaene, S., Changeux, J.-P., Naccache, L., Sackur, J., Sergent, C., 2006. Conscious, preconscious, and subliminal processing: a testable taxonomy. Trends in Cognitive Sciences 10, 204–211. https://doi.org/10.1016/j.tics.2006.03.007
Donoghue, T., Haller, M., Peterson, E.J., Varma, P., Sebastian, P., Gao, R., Noto, T., Lara, A.H., Wallis, J.D., Knight, R.T., Shestyuk, A., Voytek, B., 2020. Parameterizing neural power spectra into periodic and aperiodic components. Nat Neurosci 23, 1655–1665. https://doi.org/10.1038/s41593-020-00744-x
Dou, W., Morrow, A., Iemi, L., Samaha, J., 2022. Pre-stimulus alpha-band phase gates early visual cortex responses. NeuroImage 253, 119060. https://doi.org/10.1016/j.neuroimage.2022.119060
Dugue, L., Marque, P., VanRullen, R., 2011. The Phase of Ongoing Oscillations Mediates the Causal Relation between Brain Excitation and Visual Perception. Journal of Neuroscience 31, 11889–11893. https://doi.org/10.1523/JNEUROSCI.1161-11.2011
Fakche, C., VanRullen, R., Marque, P., Dugué, L., 2022. α Phase-Amplitude Tradeoffs Predict Visual Perception. eNeuro 9, ENEURO.0244-21.2022. https://doi.org/10.1523/ENEURO.0244-21.2022
Ferrè, E.R., Sahani, M., Haggard, P., 2016. Subliminal stimulation and somatosensory signal detection. Acta Psychologica 170, 103–111. https://doi.org/10.1016/j.actpsy.2016.06.009
Fiebelkorn, I.C., Foxe, J.J., Butler, J.S., Mercier, M.R., Snyder, A.C., Molholm, S., 2011. Ready, Set, Reset: Stimulus-Locked Periodicity in Behavioral Performance Demonstrates the Consequences of Cross-Sensory Phase Reset. Journal of Neuroscience 31, 9971–9981. https://doi.org/10.1523/JNEUROSCI.1338-11.2011
Fiebelkorn, I.C., Kastner, S., 2019. A Rhythmic Theory of Attention. Trends in Cognitive Sciences 23, 87–101. https://doi.org/10.1016/j.tics.2018.11.009
Forschack, N., Nierhaus, T., Müller, M.M., Villringer, A., 2020. Dissociable neural correlates of stimulation intensity and detection in somatosensation. NeuroImage 217, 116908. https://doi.org/10.1016/j.neuroimage.2020.116908
Gruber, W.R., 2005. Alpha Phase Synchronization Predicts P1 and N1 Latency and Amplitude Size. Cerebral Cortex 15, 371–377. https://doi.org/10.1093/cercor/bhh139
Haegens, S., Cousijn, H., Wallis, G., Harrison, P.J., Nobre, A.C., 2014. Inter- and intra-individual variability in alpha peak frequency. NeuroImage 92, 46–55. https://doi.org/10.1016/j.neuroimage.2014.01.049
Hämäläinen, M., Hari, R., Ilmoniemi, R.J., Knuutila, J., Lounasmaa, O.V., 1993. Magnetoencephalography—theory, instrumentation, and applications to noninvasive studies of the working human brain. Rev. Mod. Phys. 65, 413–497. https://doi.org/10.1103/RevModPhys.65.413
Han, B., Zhang, Y., Shen, L., Mo, L., Chen, Q., 2023. Task demands modulate pre-stimulus alpha frequency and sensory template during bistable apparent motion perception. Cerebral Cortex 33, 1679–1692. https://doi.org/10.1093/cercor/bhac165
Han, L., Liang, Z., Jiacai, Z., Changming, W., Li, Y., Xia, W., Xiaojuan, G., 2015. Improving N1 classification by grouping EEG trials with phases of pre-stimulus EEG oscillations. Cogn Neurodyn 9, 103–112. https://doi.org/10.1007/s11571-014-9317-x
Hansen, P.C., Kringelbach, M.L., Salmelin, R. (Eds.), 2010. MEG: an introduction to methods. Oxford University Press, New York.
Hanslmayr, S., Volberg, G., Wimber, M., Dalal, S.S., Greenlee, M.W., 2013. Prestimulus Oscillatory Phase at 7 Hz Gates Cortical Information Flow and Visual Perception. Current Biology 23, 2273–2278. https://doi.org/10.1016/j.cub.2013.09.020
Hari, R., Parkkonen, L., Nangini, C., 2010. The brain in time: insights from neuromagnetic recordings. Annals of the New York Academy of Sciences 1191, 89–109. https://doi.org/10.1111/j.1749-6632.2010.05438.x
Harris, A.M., 2023. Phase resets undermine measures of phase-dependent perception. Trends in Cognitive Sciences 27, 224–226. https://doi.org/10.1016/j.tics.2022.12.008

Harter, M.R., 1967. Excitability cycles and cortical scanning: A review of two hypotheses of central intermittency in perception. Psychological Bulletin 68, 47–58. https://doi.org/10.1037/h0024725
Iemi, L., Chaumon, M., Crouzet, S.M., Busch, N.A., 2017. Spontaneous Neural Oscillations Bias Perception by Modulating Baseline Excitability. J. Neurosci. 37, 807–819. https://doi.org/10.1523/JNEUROSCI.1432-16.2016
Ikumi, N., Torralba, M., Ruzzoli, M., Soto-Faraco, S., 2019. The phase of pre-stimulus brain oscillations correlates with cross-modal synchrony perception. Eur J Neurosci 49, 150–164. https://doi.org/10.1111/ejn.14186
Iliopoulos, F., Taskin, B., Villringer, A., Nierhaus, T., 2020. Imperceptible Somatosensory Single Pulse and Pulse Train Stimulation Oppositely Modulate Mu Rhythm Activity and Perceptual Performance. Cerebral Cortex 30, 6284–6295. https://doi.org/10.1093/cercor/bhaa185
Jensen, O., Mazaheri, A., 2010. Shaping Functional Architecture by Oscillatory Alpha Activity: Gating by Inhibition. Front. Hum. Neurosci. 4. https://doi.org/10.3389/fnhum.2010.00186
Johannknecht, M., Kayser, C., 2022. The influence of the respiratory cycle on reaction times in sensory-cognitive paradigms. Sci Rep 12, 2586. https://doi.org/10.1038/s41598-022-06364-8
Johannknecht, M., Schnitzler, A., Lange, J., 2024. Prestimulus alpha phase modulates visual temporal integration. eNeuro 11 (9). https://doi.org/10.1523/ENEURO.0471-23.2024
Johannknecht, M., Schnitzler, A., Lange, J., 2025. Subliminal visual stimuluation produces behavioral oscillations in mutliple frequencies in a visual integration task. Sci Rep 15 2531 (2025). https://doi.org/10.1038/s41598-025-85385-5
Keil, J., Senkowski, D., 2017. Individual Alpha Frequency Relates to the Sound-Induced Flash Illusion. Multisens Res 30, 565–578. https://doi.org/10.1163/22134808-00002572
Keitel, C., Ruzzoli, M., Dugué, L., Busch, N.A., Benwell, C.S.Y., 2022. Rhythms in cognition: The evidence revisited. Eur J of Neuroscience 55, 2991–3009. https://doi.org/10.1111/ejn.15740
Kim, K., Ladenbauer, J., Babo-Rebelo, M., Buot, A., Lehongre, K., Adam, C., Hasboun, D., Lambrecq, V., Navarro, V., Ostojic, S., Tallon-Baudry, C., 2019. Resting-State Neural Firing Rate Is Linked to Cardiac-Cycle Duration in the Human Cingulate and Parahippocampal Cortices. J. Neurosci. 39, 3676–3686. https://doi.org/10.1523/JNEUROSCI.2291-18.2019
Kluger, D.S., Balestrieri, E., Busch, N.A., Gross, J., 2021. Respiration aligns perception with neural excitability. eLife 10, e70907. https://doi.org/10.7554/eLife.70907
Krasich, K., Simmons, C., O'Neill, K., Giattino, C.M., De Brigard, F., Sinnott-Armstrong, W., Mudrik, L., Woldorff, M.G., 2022. Prestimulus oscillatory brain activity interacts with evoked recurrent processing to facilitate conscious visual perception. Sci Rep 12, 22126. https://doi.org/10.1038/s41598-022-25720-2
Kraut, A.T.A., Albrecht, T., 2022. Neural correlates of temporal integration and segregation in metacontrast masking: A phenomenological study. Psychophysiology n/a, e14085. https://doi.org/10.1111/psyp.14085
Lakatos, P., Chen, C.-M., O'Connell, M.N., Mills, A., Schroeder, C.E., 2007. Neuronal Oscillations and Multisensory Interaction in Primary Auditory Cortex. Neuron 53, 279–292. https://doi.org/10.1016/j.neuron.2006.12.011
Landau, A.N., Fries, P., 2012a. Attention Samples Stimuli Rhythmically. Current Biology 22, 1000–1004. https://doi.org/10.1016/j.cub.2012.03.054
Landau, A.N., Fries, P., 2012b. Attention Samples Stimuli Rhythmically. Current Biology 22, 1000–1004. https://doi.org/10.1016/j.cub.2012.03.054
Lange, J., Oostenveld, R., Fries, P., 2013. Reduced Occipital Alpha Power Indexes Enhanced Excitability Rather than Improved Visual Perception. Journal of Neuroscience 33, 3212–3220. https://doi.org/10.1523/JNEUROSCI.3755-12.2013
Limbach, K., Corballis, P.M., 2016. Prestimulus alpha power influences response criterion in a detection task: Prestimulus alpha power influences response. Psychophysiol 53, 1154–1164. https://doi.org/10.1111/psyp.12666
Liu, X., Melcher, D., 2023. The effect of familiarity on behavioral oscillations in face perception. Sci Rep 13, 10145. https://doi.org/10.1038/s41598-023-34812-6
Makeig, S., Westerfield, M., Jung, T.-P., Enghoff, S., Townsend, J., Courchesne, E., Sejnowski, T.J., 2002. Dynamic Brain Sources of Visual Evoked Responses. Science 295, 690–694. https://doi.org/10.1126/science.1066168
Manassi, M., Sayim, B., Herzog, M.H., 2013. When crowding of crowding leads to uncrowding. Journal of Vision 13, 10–10. https://doi.org/10.1167/13.13.10
Maris, E., Oostenveld, R., 2007. Nonparametric statistical testing of EEG- and MEG-data. Journal of Neuroscience Methods 164, 177–190. https://doi.org/10.1016/j.jneumeth.2007.03.024

Mathewson, K.E., Gratton, G., Fabiani, M., Beck, D.M., Ro, T., 2009. To See or Not to See: Prestimulus Phase Predicts Visual Awareness. Journal of Neuroscience 29, 2725–2732. https://doi.org/10.1523/JNEUROSCI.3963-08.2009

Mazaheri, A., Jensen, O., 2006. Posterior α activity is not phase-reset by visual stimuli. Proc. Natl. Acad. Sci. U.S.A. 103, 2948–2952. https://doi.org/10.1073/pnas.0505785103

Mazaheri, A., Picton, T.W., 2005. EEG spectral dynamics during discrimination of auditory and visual targets. Cognitive Brain Research 24, 81–96. https://doi.org/10.1016/j.cogbrainres.2004.12.013

Melcón, M., Stern, E., Kessel, D., Arana, L., Poch, C., Campo, P., Capilla, A., 2023. Perception of near-threshold visual stimuli is influenced by pre-stimulus alpha-band amplitude but not by alpha phase (preprint). Neuroscience. https://doi.org/10.1101/2023.03.14.532551

Merholz, G., Grabot, L., VanRullen, R., Dugué, L., 2022. Periodic attention operates faster during more complex visual search. Sci Rep 12, 6688. https://doi.org/10.1038/s41598-022-10647-5

Michail, G., Toran Jenner, L., Keil, J., 2022. Prestimulus alpha power but not phase influences visual discrimination of long-duration visual stimuli. Eur J of Neuroscience 55, 3141–3153. https://doi.org/10.1111/ejn.15169

Migliorati, D., Zappasodi, F., Perrucci, M.G., Donno, B., Northoff, G., Romei, V., Costantini, M., 2020. Individual Alpha Frequency Predicts Perceived Visuotactile Simultaneity. Journal of Cognitive Neuroscience 32, 1–11. https://doi.org/10.1162/jocn_a_01464

Milton, A., Pleydell-Pearce, C.W., 2016. The phase of pre-stimulus alpha oscillations influences the visual perception of stimulus timing. NeuroImage 133, 53–61. https://doi.org/10.1016/j.neuroimage.2016.02.065

Minami, S., Amano, K., 2017. Illusory Jitter Perceived at the Frequency of Alpha Oscillations. Current Biology 27, 2344-2351.e4. https://doi.org/10.1016/j.cub.2017.06.033

Mishkin, M., Ungerleider, L.G., Macko, K.A., 1983. Object vision and spatial vision: two cortical pathways. Trends in Neurosciences 6, 414–417. https://doi.org/10.1016/0166-2236(83)90190-X

Monto, S., Palva, S., Voipio, J., Palva, J.M., 2008. Very Slow EEG Fluctuations Predict the Dynamics of Stimulus Detection and Oscillation Amplitudes in Humans. J. Neurosci. 28, 8268–8272. https://doi.org/10.1523/JNEUROSCI.1910-08.2008

Mooneyham, B.W., Schooler, J.W., 2013. The costs and benefits of mind-wandering: A review. Canadian Journal of Experimental Psychology / Revue canadienne de psychologie expérimentale 67, 11–18. https://doi.org/10.1037/a0031569

Mudrik, L., Deouell, L.Y., 2022. Neuroscientific Evidence for Processing Without Awareness. Annu. Rev. Neurosci. 45, 403–423. https://doi.org/10.1146/annurev-neuro-110920-033151

Nierhaus, T., Forschack, N., Piper, S.K., Holtze, S., Krause, T., Taskin, B., Long, X., Stelzer, J., Margulies, D.S., Steinbrink, J., Villringer, A., 2015. Imperceptible Somatosensory Stimulation Alters Sensorimotor Background Rhythm and Connectivity. J. Neurosci. 35, 5917–5925. https://doi.org/10.1523/JNEUROSCI.3806-14.2015

Oostenveld, R., Fries, P., Maris, E., Schoffelen, J.-M., 2011. FieldTrip: Open Source Software for Advanced Analysis of MEG, EEG, and Invasive Electrophysiological Data. Computational Intelligence and Neuroscience 2011, 1–9. https://doi.org/10.1155/2011/156869

Ozdemir, R.A., Kirkman, S., Magnuson, J.R., Fried, P.J., Pascual-Leone, A., Shafi, M.M., 2022. Phase matters when there is power: Phasic modulation of corticospinal excitability occurs at high amplitude sensorimotor mu-oscillations. Neuroimage: Reports 2, 100132. https://doi.org/10.1016/j.ynirp.2022.100132

Palva, J.M., Palva, S., 2012. Infra-slow fluctuations in electrophysiological recordings, blood-oxygenation-level-dependent signals, and psychophysical time series. NeuroImage 62, 2201–2211. https://doi.org/10.1016/j.neuroimage.2012.02.060

Palva, S., 2005. Early Neural Correlates of Conscious Somatosensory Perception. Journal of Neuroscience 25, 5248–5258. https://doi.org/10.1523/JNEUROSCI.0141-05.2005

Pinel, J.P.J., Pauli, P., Barnes, S.J., 2017. Biopsychologie, 8., aktualisierte und erweiterte Auflage. ed, Ps, Psychologie. Pearson, Hallbergmoos/Germany.

Plöchl, M., Fiebelkorn, I., Kastner, S., Obleser, J., 2022. Attentional sampling of visual and auditory objects is captured by theta-modulated neural activity. Eur J of Neuroscience 55, 3067–3082. https://doi.org/10.1111/ejn.15514

Prins, N., Kingdom, F.A.A., 2018. Applying the Model-Comparison Approach to Test Specific Research Hypotheses in Psychophysical Research Using the Palamedes Toolbox. Front. Psychol. 9, 1250. https://doi.org/10.3389/fpsyg.2018.01250

Railo, H., Piccin, R., Lukasik, K.M., 2021. Subliminal perception is continuous with conscious vision and can be predicted from prestimulus electroencephalographic activity. Eur J of Neuroscience 54, 4985–4999. https://doi.org/10.1111/ejn.15354
Re, D., Inbar, M., Richter, C.G., Landau, A.N., 2019. Feature-Based Attention Samples Stimuli Rhythmically. Current Biology 29, 693-699.e4. https://doi.org/10.1016/j.cub.2019.01.010
Romei, V., Brodbeck, V., Michel, C., Amedi, A., Pascual-Leone, A., Thut, G., 2008. Spontaneous Fluctuations in Posterior -Band EEG Activity Reflect Variability in Excitability of Human Visual Areas. Cerebral Cortex 18, 2010–2018. https://doi.org/10.1093/cercor/bhm229
Romei, V., Thut, G., Mok, R.M., Schyns, P.G., Driver, J., 2012. Causal implication by rhythmic transcranial magnetic stimulation of alpha frequency in feature-based local vs. global attention: Causal role of alpha in featural attention. European Journal of Neuroscience 35, 968–974. https://doi.org/10.1111/j.1460-9568.2012.08020.x
Ruzzoli, M., Torralba, M., Morís Fernández, L., Soto-Faraco, S., 2019. The relevance of alpha phase in human perception. Cortex 120, 249–268. https://doi.org/10.1016/j.cortex.2019.05.012
Sadava, D.E., Hillis, D.M., Heller, H.C., Berenbaum, M., 2011. Biologie, 9. Auflage. ed. Spektrum, Akademischer Verlag, Heidelberg.
Samaha, J., Bauer, P., Cimaroli, S., Postle, B.R., 2015. Top-down control of the phase of alpha-band oscillations as a mechanism for temporal prediction. Proc. Natl. Acad. Sci. U.S.A. 112, 8439–8444. https://doi.org/10.1073/pnas.1503686112
Samaha, J., Postle, B.R., 2015. The Speed of Alpha-Band Oscillations Predicts the Temporal Resolution of Visual Perception. Current Biology 25, 2985–2990. https://doi.org/10.1016/j.cub.2015.10.007
Schaworonkow, N., Triesch, J., Ziemann, U., Zrenner, C., 2019. EEG-triggered TMS reveals stronger brain state-dependent modulation of motor evoked potentials at weaker stimulation intensities. Brain Stimulation 12, 110–118. https://doi.org/10.1016/j.brs.2018.09.009
Scheffer-Teixeira, R., Tort, A.B., 2016. On cross-frequency phase-phase coupling between theta and gamma oscillations in the hippocampus. eLife 5, e20515. https://doi.org/10.7554/eLife.20515
Schomer, D.L., Lopes da Silva, F.H., Niedermeyer, E. (Eds.), 2018. Niedermeyer's electroencephalography: basic principles, clinical applications, and related fields, Seventh edition. ed. Oxford University Press, New York, NY.
Schwartz, M., Rem, M.A., 1975. Does the Averaged Evoked Response Encode Subliminal Perception? Psychophysiology 12, 390–394. https://doi.org/10.1111/j.1469-8986.1975.tb00008.x
Sharp, P., Gutteling, T., Melcher, D., Hickey, C., 2022. Spatial attention tunes temporal processing in early visual cortex by speeding and slowing alpha oscillations. J. Neurosci. JN-RM-0509-22. https://doi.org/10.1523/JNEUROSCI.0509-22.2022
Silverstein, B.H., Snodgrass, M., Shevrin, H., Kushwaha, R., 2015. P3b, consciousness, and complex unconscious processing. Cortex 73, 216–227. https://doi.org/10.1016/j.cortex.2015.09.004
Song, K., Meng, M., Chen, L., Zhou, K., Luo, H., 2014. Behavioral Oscillations in Attention: Rhythmic α Pulses Mediated through θ Band. J. Neurosci. 34, 4837–4844. https://doi.org/10.1523/JNEUROSCI.4856-13.2014
Sperdin, H.F., Spierer, L., Becker, R., Michel, C.M., Landis, T., 2015. Submillisecond unmasked subliminal visual stimuli evoke electrical brain responses: VEPs to Submillisecond Unmasked Visual Stimulation. Hum. Brain Mapp. 36, 1470–1483. https://doi.org/10.1002/hbm.22716
Spieler, D., Schumacher, E. (Eds.), 2019. New Methods in Cognitive Psychology, 1st ed. Routledge. https://doi.org/10.4324/9780429318405
Tarasi, L., Romei, V., 2023. Individual Alpha Frequency Contributes to the Precision of Human Visual Processing. Journal of Cognitive Neuroscience 1–11. https://doi.org/10.1162/jocn_a_02026
Taskin, B., Holtze, S., Krause, T., Villringer, A., 2008. Inhibitory impact of subliminal electrical finger stimulation on SI representation and perceptual sensitivity of an adjacent finger. NeuroImage 39, 1307–1313. https://doi.org/10.1016/j.neuroimage.2007.09.039
Tosato, T., Rohenkohl, G., Fries, P., 2022. Performance modulations phase-locked to action depend on internal state (preprint). Neuroscience. https://doi.org/10.1101/2022.11.28.518242
Tzourio-Mazoyer, N., Landeau, B., Papathanassiou, D., Crivello, F., Etard, O., Delcroix, N., Mazoyer, B., Joliot, M., 2002. Automated Anatomical Labeling of Activations in SPM Using a Macroscopic Anatomical Parcellation of the MNI MRI Single-Subject Brain. NeuroImage 15, 273–289. https://doi.org/10.1006/nimg.2001.0978
Uhlhaas, P.J., Liddle, P., Linden, D.E.J., Nobre, A.C., Singh, K.D., Gross, J., 2017. Magnetoencephalography as a Tool in Psychiatric Research: Current Status and Perspective. Biological Psychiatry: Cognitive Neuroscience and Neuroimaging 2, 235–244. https://doi.org/10.1016/j.bpsc.2017.01.005

Valera, F.J., Toro, A., Roy John, E., Schwartz, E.L., 1981. Perceptual framing and cortical alpha rhythm. Neuropsychologia 19, 675–686. https://doi.org/10.1016/0028-3932(81)90005-1
van Dijk, H., Schoffelen, J.-M., Oostenveld, R., Jensen, O., 2008. Prestimulus Oscillatory Activity in the Alpha Band Predicts Visual Discrimination Ability. Journal of Neuroscience 28, 1816–1823. https://doi.org/10.1523/JNEUROSCI.1853-07.2008
VanRullen, R., 2016a. Perceptual Cycles. Trends in Cognitive Sciences 20, 723–735. https://doi.org/10.1016/j.tics.2016.07.006
VanRullen, R., 2016b. How to Evaluate Phase Differences between Trial Groups in Ongoing Electrophysiological Signals. Front. Neurosci. 10. https://doi.org/10.3389/fnins.2016.00426
VanRullen, R., Koch, C., 2003. Is perception discrete or continuous? Trends in Cognitive Sciences 7, 207–213. https://doi.org/10.1016/S1364-6613(03)00095-0
Venskus, A., Ferri, F., Migliorati, D., Spadone, S., Costantini, M., Hughes, G., 2021. Temporal binding window and sense of agency are related processes modifiable via occipital tACS. PLoS ONE 16, e0256987. https://doi.org/10.1371/journal.pone.0256987
Venskus, A., Hughes, G., 2021. Individual differences in alpha frequency are associated with the time window of multisensory integration, but not time perception. Neuropsychologia 159, 107919. https://doi.org/10.1016/j.neuropsychologia.2021.107919
Voytek, B., 2010. Shifts in gamma phase–amplitude coupling frequency from theta to alpha over posterior cortex during visual tasks. Front. Hum. Neurosci. 4. https://doi.org/10.3389/fnhum.2010.00191
Vrba, J., Robinson, S.E., 2001. Signal Processing in Magnetoencephalography. Methods 25, 249–271. https://doi.org/10.1006/meth.2001.1238
Wu, C.-T., Busch, N.A., Fabre-Thorpe, M., VanRullen, R., 2009. The Temporal Interplay between Conscious and Unconscious Perceptual Streams. Current Biology 19, 2003–2007. https://doi.org/10.1016/j.cub.2009.10.017
Wutz, A., Melcher, D., Samaha, J., 2018. Frequency modulation of neural oscillations according to visual task demands. Proc. Natl. Acad. Sci. U.S.A. 115, 1346–1351. https://doi.org/10.1073/pnas.1713318115
Wutz, A., Muschter, E., van Koningsbruggen, M.G., Weisz, N., Melcher, D., 2016. Temporal Integration Windows in Neural Processing and Perception Aligned to Saccadic Eye Movements. Current Biology 26, 1659–1668. https://doi.org/10.1016/j.cub.2016.04.070
Zazio, A., Ruhnau, P., Weisz, N., Wutz, A., 2022. Pre-stimulus alpha-band power and phase fluctuations originate from different neural sources and exert distinct impact on stimulus-evoked responses. Eur J of Neuroscience 55, 3178–3190. https://doi.org/10.1111/ejn.15138

Eidesstattliche Erklärung

Ich versichere an Eides Statt, dass die Dissertation von mir selbständig und ohne unzulässige fremde Hilfe unter Beachtung der „Grundsätze zur Sicherung guter wissenschaftlicher Praxis an der Heinrich-Heine-Universität Düsseldorf“ erstellt worden ist. Die Dissertation wurde in der vorliegenden oder in ähnlicher Form noch bei keiner anderen Institution eingereicht. Ich habe bisher keine erfolglosen Promotionsversuche unternommen.

Düsseldorf, den

Michelle Johannknecht

Danksagung

Ich möchte diese Zeilen nutzen, um mich bei all meinen Freunden/Freundinnen, Familie und Kollegen/Kolleginnen bedanken, die mich auf dieser Reise begleitet haben. Für mich ist das Erlangen, dieses akademischen Grades kein Beweis für mein Können und/oder Wissen, sondern ein Nachweis für meine persönliche Entwicklung, die ich in dieser Zeit erlebt habe. Daher möchte ich mich nicht für den intellektuellen Austausch bedanken, sondern für die schönen Erfahrungen und Erinnerungen, die ich in der Zeit meines PhDs erlebt habe.

Auch wenn ich mir recht sicher bin, dass nur eine Handvoll Menschen diese Danksagung lesen werde, so möchte ich doch diese Worte loswerden: Einen akademischen Grad definiert keine Person. Das Wissen, das man erlangt hat, nebenbei, welches nicht messbar ist durch irgendwelche Publikationen oder Noten, ist das, was einen ausmachen sollte. Es ist die persönliche Entwicklung, die man jeden Tag auf neue erlebt, die wichtig für ein sollte. Man sollte stolz zurückblicken können und erkennen können, dass man selbst dazu in der Lage war, das Geschaffte zu erreichen und das ist nicht der Titel, den man trägt, sondern den Weg, den man gegangen ist.

Es kann viele Bürden und Umwege geben, doch dies sind nur Zeichen von persönlicher Stärke, die man aufgebracht hat, um diese Hindernisse zu überwinden. So kann ich also als abschließende Worte sagen: Nein ich bin nicht stolz auf den akademischen Titel, den ich nun bald tragen werde, sondern ich bin stolz, dass ich diesen Weg gegangen bin, dass ich es geschafft habe, die Stärke aufzubringen und meine persönlichen Hindernisse überwunden habe. Darauf bin ich stolz, nicht auf den Title den ich tragen darf.

Appendix

Contribution

Study One: Prestimulus alpha phase modulates visual temporal integration

Michelle Johannknecht: Performed research, analysed the data and wrote the manuscript

Prof. Dr. Alfons Schnitzler: Wrote the manuscript

PD Dr. Joachim Lange: Conceptualized research, analysed the data and wrote the manuscript

Published in eNeuro 12th August 2024

Impact factor (2022): 3.4

Study Two: Subliminal visual stimulation produces broadband behavioural oscillations in a visual integration task

Michelle Johannknecht: Conceptualized research, performed research, analysed the data and wrote the manuscript

Prof. Dr. Alfons Schnitzler: Wrote the manuscript

PD Dr. Joachim Lange: Wrote the manuscript

Published in Scientific Reports 20th January 2025

Impact factor (2022): 4.6

Supplementary Material

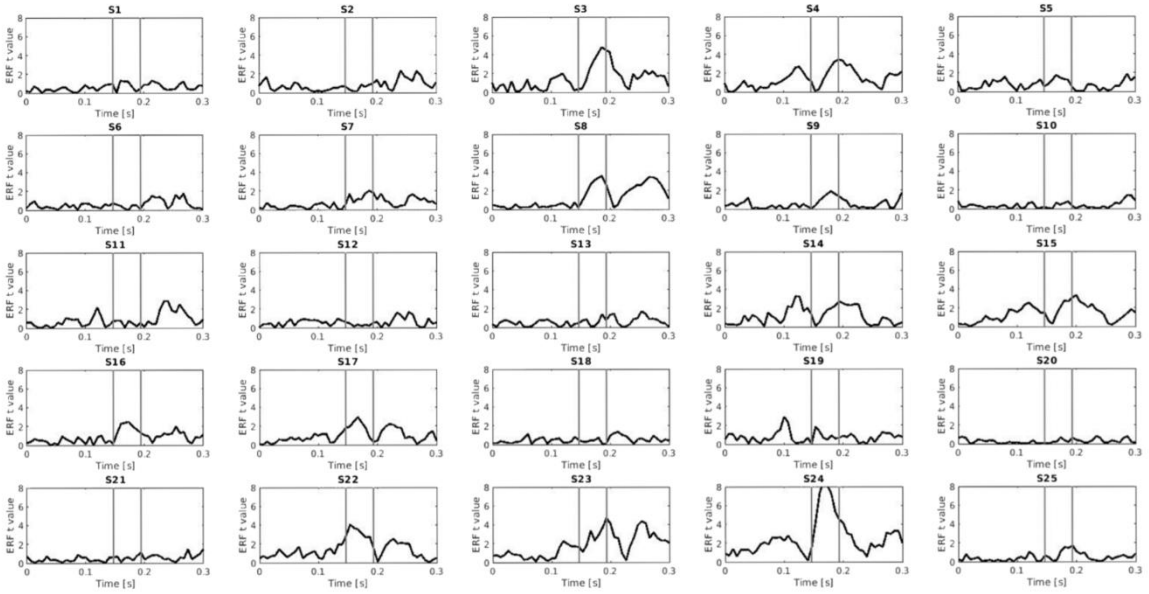

Figure S1 Individual ERF amplitude. Subplots show the individual ERF amplitude (black line) for each subject. Y-axis shows absolute ERF t-values and x-axis time in seconds. Grey lines indicate analysis window for N170 peak analysis.